Benthic foraminiferal proxies of environmental changes during the pre-Messinian salinity crisis of the Sinis Basin (W Sardinia, Mediterranean Sea)

Carla Buosi [a,*], Antonietta Cherchi [a] and Davide Mana [b]

[a] Dipartimento di Scienze Chimiche e Geologiche, Università degli Studi di Cagliari, I-09127 Cagliari, Italy.

[b] Via Mazzini 7, Castelnuovo Belbo, I-14043, Asti, Italy

* Corresponding author: Carla Buosi, e-mail: cbuosi@unica.it

Abstract

The Messinian succession cropping out in a marginal basin of the Mediterranean Sea (Sinis Basin, W Sardinia) was studied in its benthic foraminiferal content in order to investigate the main palaeoenvironmental changes occurring. A shallowing upward depositional trend, from an upper bathyal-circalittoral environment to a coastal lagoon, was recognized during the pre-Messinian Salinity Crisis. In the lower part of the analysed succession (Capo San Marco Formation), upper bathyal-circalittoral conditions are suggested by species with a wide depth-range, such as *Cibicidoides pseudoungerianus, Melonis pompilioides, Oridorsalis umbonatus,* bolivinids and buliminids. In the middle part of this formation, the progressively shallowing environment is indicated by the low abundance of planktonics coupled with the upward increase of shallow-water epiphytic species (*Lobatula lobatula, Elphidium crispum, E. macellum, Ammonia beccarii, Hanzawaia boueana*). The progressive marine restriction led to the development of hypohaline conditions typical of lagoonal environments as suggested by *Ammonia tepida* and oligotypic macrofaunas. The succession stops with the deposition of laminated limestones barren in fossils (Sinis Laminated Limestone Formation).

A mixed siliciclastic-carbonate platform (Torre del Sevo Formation), characterized by fluvial deposits intercalated in the marine succession, developed as suggested by benthic foraminifera, ostracods, very rare planktonic species and macrofaunas.

Sinis Laminated Limestone Formation and Torre del Sevo Formation constituted part of the Terminal Carbonate Complex, strongly eroded by the Messinian Erosional Surface (MES) at its top. The palaeoecological conditions in the Sinis Basin were intermittently suitable for sustaining full-marine biota, indicating that this marginal basin was not constantly desiccated during the pre-Messinian salinity crisis.

Keywords: benthic foraminifera; palaeoenvironments; Messinian Salinity Crisis; Sardinian marginal basin; western Mediterranean.

1. Introduction

At the end of the Miocene, major palaeoceanographic and environmental changes occurred in the Mediterranean basin as a consequence of the closure of gateways connecting the Atlantic and the Mediterranean (Roveri et al., 2014 and references therein). The absence of this connection coupled with a strong evaporation caused the progressive desiccation of the Mediterranean basin and a massive salinity crisis (Rouchy and Caruso, 2006; Manzi et al., 2013; Roveri et al., 2014; Flecker et al., 2015). During the interval that anticipates the Messinian Salinity Crisis (pre-MSC), the Mediterranean and Atlantic were probably connected through the Iberian or Betic portal (Southern Spain), and the Rifian corridor in Northern Morocco (Roveri et al., 2014). The timing of closure of these corridors is still subject to significant uncertainty (Roveri et al., 2014). A study by Pérez-Asensio et al. (2012a) has placed the timing of the Betic portal closure to around 6.2 Ma, whereas the Rifian Corridor was emerged at about 6.0 Ma (Krijgsman et al., 1999b). However, some authors (Meijer and Krijgsman, 2005) suggested that the influxes of Atlantic waters in the Mediterranean Sea through a very shallow and narrow connection cannot be excluded.

The first hypothesis of a Messinian Salinity Crisis - MSC (Selli, 1954) was defined after the recognition of coeval, widespread development of hyper- and hypohaline conditions and the deposition of evaporitic

successions all around the Mediterranean (Ogniben, 1957; Selli, 1960; Ruggieri, 1967), which demonstrated the occurrence of extreme conditions at the end of the Miocene. The Deep Sea Drilling Project Leg 13 (Hsü, 1972, 1973; Hsü et al., 1973a,b) confirmed this concept of a MSC due to the discovery of the evaporitic subsurface units in the deep basins of the Mediterranean Sea (e.g., Ryan, 2009; Roveri et al., 2014). The Early Messinian stage (pre-MSC; 7.251–5.97 Ma) is a pre-conditioning phase of the MSC characterized by changes in water chemistry and deterioration of paleoenvironmental conditions. These changes occurred progressively and parallel to the gradual restriction of the Atlantic-Mediterranean gateway and leading to the deposition of evaporites in marginal basins (Roveri et al., 2014).

Numerous studies in the Mediterranean area of time intervals before, during and after the Messinian Salinity Crisis have been carried out using a multidisciplinary approach (e.g., Krijgsman et al., 1999a; Rouchy and Caruso, 2006; Bache et al., 2012). Several studies have focused on palaeoceanographic evolution (e.g., Kouwenhoven et al., 1999, 2003; Gennari et al., 2013; Pérez-Asensio et al., 2014), palaeoclimatic and glacio-eustatic changes (e.g., Sierro et al., 1999; Hilgen et al., 2007), in addition to biofacies analysis and sedimentary models (e.g., Aguirre and Sánchez-Almazo, 2004; Braga et al., 2006; Caruso et al., 2015), integrated high-resolution stratigraphy (e.g., Gorini et al., 2015; Hilgen et al., 2000a,b; Morigi et al., 2007) and palaeoenvironmental recostruction (e.g., Sánchez-Almazo et al., 2001; Kouwenhoven et al., 2006; Pérez-Asensio et al., 2012b; Violanti et al., 2013). However, there is still an intense debate about the interpretation and correlation of palaeoenvironmental changes in the onshore marginal basins that have been supposed to have a palaeobathymetry ranging between <200 m (shallow-water) and >1000 m (deep-water; see Roveri et al., 2014). Furthermore, local conditions (e.g., vertical movements of the substrate) can play a role in depositional processes of marginal basins during Messinian and these factors should be taken into account when comparisons are made with other sites. As a result, there is still considerable uncertainty about some key aspects of the MSC in marginal basins, such as salinity fluctuation and reflooding episodes (e.g., Riding et al., 1998; Braga et al., 2006). The impact of the MSC on Mediterranean marine ecosystems, which is related to the restriction of connection to the Atlantic and the progressive deterioration of environmental conditions, plays an important role in the distribution of both planktonic and benthic species. The palaeoenvironmental

changes recorded by benthic foraminiferal assemblages in pre-evaporitic and evaporitic successions, and the impact of the MSC on foraminiferal diversity, have been investigated by several authors in other Mediterranean marginal basins (e.g., Goubert et al., 2001; Kouwenhoven et al., 2006; Drinia et al., 2007; Di Stefano et al., 2010).

In this paper, we present new results of the palaeoenvironmental changes occurring in the marginal Sinis Basin (western Sardinia) through a quantitative micropalaeontological analysis of benthic foraminiferal assemblages. Our investigation allowed us to recognize a shallowing upward depositional trend, from an upper bathyal-circalittoral environment to a coastal lagoon during the pre-Messinian Salinity Crisis. The micropaleontological content in the Sinis Basin indicated that this marginal basin was not constantly desiccated during the pre-Messinian salinity crisis and the palaeoecological conditions were intermittently suitable for sustaining full-marine biota. In addition, previous data on calcareous nannofossils and planktonic foraminifera (Cherchi and Martini, 1981; Cherchi et al., 1985) have been used for the chronostratigraphic calibration of the palaeoecological events, in order to compare our palaeoenvironmental reconstruction with data from other Messinian marginal basins.

2. Study area

2.1 Geological setting

The Cenozoic history of the Corsica-Sardinian Block is closely linked to the geodynamic evolution of the western Mediterranean (Cherchi and Montadert, 1982). The Sardinian Graben-System began in a continental environment before the Oligo-Miocene transgression, which was controlled by tensional tectonic and Cenozoic volcanic activity. A Messinian compressional event (NE-SW oriented) strongly affected the Oligo-Miocene Graben-System producing inversion structures (Casula et al., 2001). The Sinis marginal Basin (Fig. 1) is located on the northern edge of the Campidano Plio-Quaternary Graben and is bounded by an east-dipping master fault, at East of Capo San Marco (Casula et al., 2001).

The Cenozoic units outcropping in the Sinis peninsula are as follows (Fig. 1): (a) Oligo-Miocene volcano-sedimentary complex; (b) Aquitanian to Messinian marine sediments; (c) Zanclean

transgressive marls; (d) Pliocene basaltic flows, dated at 4.83-4.58, 3.28-3.18 Ma (Duncan et al., 2011), and previously at 3.12-3.04 Ma (Montigny et al., 1981); and (e) Pleistocene aeolianites.

2.2 Upper Miocene succession

Four lithostratigraphic units have been recognized in the uppermost Tortonian-Messinian succession from Capo San Marco (Section A) and M. Palla (Section B; Fig. 1): (a) the hemipelagic Basal Marl (BM); (b) the Capo San Marco Formation (CSMF), consisting predominantly of fossiliferous sandy marls and marly limestones, including microbial mounds and microbialithic crusts; (c) the Sinis Laminated Limestone Formation (SLLF), which is composed of azoic thin-bedded micritic limestones; and (d) the Torre del Sevo Formation (TSF) consisting of karstified and brecciated marine limestones and dolostones.

The Basal Marl (BM) formation contains frequent to abundant calcareous nannofossils and foraminifera (Cherchi and Martini, 1981), as well as diversified macrofaunas (including *Amussium* sp., *Dentalium* sp., *Pycnodonte navicularis*), echinids and brachiopods, indicating an upper bathyal zone. The upper part of the BM unit (Fig. 1) consists of silty marls containing two thin, sapropelitic beds with framboidal pyrite crystals and pyritized moulds of benthic foraminifera, indicating stagnant conditions at the sea bottom (Cherchi and Martini, 1981).

A normal fault separates the BM unit from the overlying Capo San Marco Formation (CSMF; Fig. 1). The lower part of the CSMF includes microbial-bryozoan mounds that developed in muddy-silty sediments (Moissette et al., 2002; André et al., 2004; Saint Martin, 2010). These build-ups exhibit a thrombolytic fabric and are associated with serpulid and bryozoan colonies. Laterally, small pockets, infilled by laminated clayey marls bearing articulated and iso-oriented shallow water bivalves and ostracods (*Cytheridea*, *Callistocythere*, *Aurila* and epiphytic *Xestoleberis*), have been recognized (Cherchi et al., 1985). The microbialithic mounds are followed by a biosiliceous episode containing diatomitic oozes and radiolarians, overlain by a yellowish clay bearing interbedded shell-layers and by bioturbated silty marls with pectinids, stenohaline faunas (irregular echinoids), calcareous nannofossils, and planktonic and benthic foraminifera. The middle part of the CSMF (from 8 m to 14 m; Fig. 1) contains yellowish mudstones (S16, S17, S19-S23, S25-S28), bearing unarticulated shells of venerids

and cardiids (*Acanthocardia paucicostata*), indicating a low-energy sublittoral environment alternated with mollusc-rich bioturbated packstone (S15 at about 7.5 m and S18 at about 9.5 m). The upper part of the CSMF consists of muddy siltstones (S24, S29) and clayey marls (S31, S32) that sometimes contain articulated mytilids, pectinids, stenohaline echinoids, gobiid otoliths and ostracods (*Ruggieria*, *Incongruellina* and *Macrocypris;* Cherchi et al., 1985), indicating marine flooding episodes. Two continental episodes (montmorillonitic pockets, 20 to 40 cm thick; P in Fig. 1) are exposed respectively below and above hard limestone beds containing articulated mitilids and *Corbula gibba* (bivalve) community. The last subaerial deposits (Fig. 2A) are directly overlain by thin-bedded azoic micritic limestones (SLLF). According to André et al. (2004), from the BM up to SLLF, one and a half major cycle of progradation–retrogradation are shown prior to the deposition of the TSF (Fig. 2A).

The Sinis Laminated Limestone Formation (SLLF) consists of a monotonous succession of white, thinly-bedded, azoic micrites, showing a cyclical deposition (Fig. 2B). This formation is widely exposed along the western vertical cliff of the Sinis Peninsula (Fig. 3), showing a thickness of about 10÷15 m. SEM analyses performed by André et al. (2004) reveal a microcrystalline texture, while X-ray diffraction indicates that more than 95% is calcite. This is comparable to the 96% calcium carbonate found by Cherchi et al. (1978). Rarely tiny shell debris are clearly distinguishable between the micritic beds. At the Capo San Marco section, only 6 m of the SLLF are exposed, because of the strong pre-basaltic erosion. At the Monte Palla (Section B, Fig. 1), this unit is interrupted by an erosional subaerial surface, followed by the unconformable deposition of the TSF, suggesting an unclear chronostratigraphic hiatus (H in Fig. 1).

The Torre del Sevo Formation (TSF) is constituted of a siliciclastic-carbonate marine platform containing several subaerial episodes marked by paleosoil deposits (P; Fig. 1). According to Cornée et al. (2008) this unit belongs to the Terminal Carbonate Complex (TCC). The lower part consists of marine deposits (sandy marls, marly-limestones) bearing stenohaline biota: bivalves, echinoids, small globigerinids, and evaporitic carbonates with anhydrite nodules showing typical chickenwire structure (Cherchi et al., 1978). In the middle part (S44; Fig. 1), sands and conglomerates with rounded paleozoic clasts (quartz, schist, gneiss) reflect the regional Messinian uplift and the erosional process of the

Sardinian Variscan Basement, indicating a strong fluvial input in deltaic depositional paleoenvironments, in which marine reflooding episodes occur.

The upper part of this unit, deposited in marginal evaporitic environments (Fig. 1), is strongly fractured, karstified and brecciated, contains several oolithic levels, thin microbialithic crusts and small anhydrite nodules. At the top, the TSF is truncated by a strong subaerial erosional surface correlated to the Messinian Erosional Surface (MES), which is recognizable both onshore (Cherchi et al., 1978; André et al., 2004; Cornée et al., 2008) and offshore in seismic lines (Casula et al., 2001; Sage et al., 2005; Geletti et al., 2014; Bache et al., 2015). The karstified Messinian platform is sealed by spongolitic grey-bluish Zanclean marls. The presence of large blocks of karstified limestones that clearly belong to the TSF in the Zanclean marls documents the Messinian age for the large erosional process. The Pliocene succession covers the faulted basement referred to the compressive phase (Cherchi and Tremolieres, 1984).

2.3 Biostratigraphy

The distribution of selected planktonic foraminiferal species and calcareous nannofossils from the analyzed sections is reported from Cherchi and Martini (1981) and is summarized in Fig. 4. The inferred biochronology, based on several planktonic species is presented in Table 1.

The studied section falls under the *Globorotalia conomiozea* zone of Iaccarino (1985), corresponding to MMi 13 zone (Iaccarino et al., 2007; Fig. 4), dated at 7.246 Ma at the FO (First Occurrence) of *G. conomiozea* (included in *Globorotalia miotumida* group of Sierro et al., 1993) (Cherchi and Martini, 1981). Regarding the calcareous nannofossils, the section can be attributed to CN (Calcareous Nannoplankton) zones MNN1b/c (Raffi et al., 2003) on the basis of the co-occurrence of *Amaurolithus primus* and *Amaurolithus delicatus* from the bottom of the Sinis Messinian beds (Cherchi and Martini, 1981; Fig. 4). The nannofossils show two peak abundances of “small” *Reticulofenestra* with co-occurring peak abundances of *Helicosphaera carteri* and *Sphenolithus abies* (Cherchi and Martini, 1981).

The Global Stratotype Section and Point (GSSP) for the base of the Messinian has been defined at a level that is closely associated with the FO of the *G. miotumida* group, defined in the Oued Akrech

section (Atlantic Morocco) at 7.251 Ma, and falls within the reversed Subchron C3Br.1r (Hilgen et al., 2000a,b). The top of the Messinian is defined by the Zanclean GSSP at Eraclea Minoa (Sicily), at the base of the Trubi marls that coincide with the Pliocene reflooding of the Mediterranean and has an age of 5.33 Ma (van Couvering et al., 2000). According to Cornée et al. (2008), when comparing the stratigraphical data from the Sinis Basin with that obtained from the Melilla-Nador Basin (Morocco), the MES represents a hiatus from 5.77 to 5.3 Ma. The Erosional Surface (MES) in the Sinis Basin is sealed by Zanclean hemipelagic marls, which have been ascribed by Cherchi and Martini (1981) to the NN12 zone (*Ceratolithus tricorniculatus*) and the *Globorotalia margaritae* zone.

2.4 Previous studies

The upper Miocene deposits of Sinis Peninsula have already been the subject of historical studies. Mariani and Parona (1887) described rich diatomaceous and radiolarian assemblages that were assigned, at that time, to the Tortonian and, later on, to the Messinian (Pecorini, 1972; Cherchi, 1974). The first palaeoecological analyses of the Messinian marine faunas (bivalves, foraminifera) were carried out by Cherchi et al. (1978, 1985). The Tortonian/Messinian boundary in the Capo San Marco section was proposed by Cherchi and Martini (1981) on the basis of calcareous nannofossils and planktonic foraminifera. Microbial-bryozoan mounds, microbial patches and microbialithic crusts in lower and upper parts of the Messinian succession have been studied by Moissette et al. (2002) and André et al. (2004). According to Saint Martin (2010) these mounds contain *Girvanella*-like remains (lower part of the section) and are developed in normal marine water. The presence of a major irregular subaerial Messinian Erosional Surface (MES) on the uppermost carbonate deposits of the Sinis succession was ascribed to the Terminal Carbonate Complex (TCC; Esteban, 1979) by Cornée et al. (2008).

3. Materials and methods

Fifty samples (S1-S50; Fig. 1) were collected from the Capo San Marco Fm. (about 20 m thick, 35 samples) and Torre del Sevo Fm. (about 8 m thick; 15 samples) and analyzed in their benthic foraminiferal content. Nine of these samples were barren in the foraminiferal content. They are: S33 and

S42 (picked in the paleosoil horizons); S35, S45, S46 and S48 (from crystalline limestones); S44 (from siliciclastic sandstones); and S49 and S50 (brecciated limestones and dolostones).

Each sediment sample (about 150 g) was disaggregated and treated with H_2O_2 (10%), washed on a 63 μm sieve and dried. From each washed residue about 300 benthic foraminiferal specimens were picked, mounted on slides, taxonomically identified at the species level (when possible) and quantitatively counted. All broken tests and test fragments were interpreted as transported and/or reworking and not included in the count. The counts have been expressed as percentages, representing the relative abundance of each taxon in the assemblages. Benthic foraminifera were identified following the generic classifications of Loeblich and Tappan (1987) and other taxonomic works (e.g., Cimerman and Langer, 1991; Debenay, 2012; Hottinger et al., 1993; Milker and Schmiedl, 2012; Sgarrella and Moncharmont Zei, 1993). The relative abundance of the most significant benthic foraminiferal species along the studied succession is reported in Fig. 5. The most abundant benthic species (all the species occurring with a relative abundance ≥3% and that were present in at least three samples of the succession) were grouped in three categories according to analysis of the ecological preferences of the dominant species (see Appendix A): potential epiphytes, nutrient-enriched conditions species and potential low salinity species. This subdivision shows some limitations because certain species can exhibit different life styles. For example, *Lobatula lobatula* is not exclusively linked to vegetation but it can also be attached to hard substrate such as shells (Murray, 1991). *Ammonia beccarii* is found as epiphytes in the Mediterranean basin (Mateu-Vicens et al., 2014) but it is reported as shallow infaunal dwelling in sandy to muddy substrates (e.g., Debenay et al., 1998; Goineau et al., 2015). In addition, several low-salinity species can be also found in normal-marine waters (like *Elphidium macellum* and *Haynesina germanica*). In spite of these limitations, this subdivision can be used to infer general environmental information.

Several diversity indices were calculated using the PAST statistical software (Hammer et al., 2001): species richness (S, number of species), the Shannon index (H, Shannon and Weaver, 1963) and dominance (D). The foraminiferal density (FD, number of specimens per 5 cm^3 of sediment) was also calculated. The distribution pattern of each diversity index along the studied succession together with the curves representing the ecological groups previously defined are in Fig. 6.

Multivariate statistical techniques of Q-mode Hierarchical Cluster Analysis (HCA) and Principal Component Analysis (PCA) were performed using the PAST statistical software (Hammer et al., 2001). Only the 23 species that were more abundant than 3% in at least three samples were considered for the statistical treatment. The HCA was based on Euclidean-distance correlation coefficients in order to measure similarities, whereas on the Ward's linkage method to arrange pairs and groups into hierarchic dendrograms. The PCA was carried out to determine which species were influencing the formation of clusters.

4. Results

4.1 Benthic foraminiferal assemblages

The benthic foraminiferal assemblages were largely dominated by hyaline species and subordinately by porcelanaceous and agglutinated species. In total, 62 benthic foraminiferal species, belonging to 40 genera, were identified (Appendix B). The relative abundances highly varied along the succession and from sample to sample, with 23 species showing relative abundances greater than 3% in at least three samples (Fig. 5). The most frequent species were: *A. beccarii*, *A. tepida*, *Bolivina arta*, *B. dilatata*, *Bulimina aculeata*, *B. echinata*, *Cibicidoides pseudoungerianus*, *Elphidium crispum*, *E. macellum*, *Hanzawaia boueana*, *H. germanica*, *L. lobatula*, and *Melonis pompilioides.* Among the most frequent species, *A. tepida* and *A. beccarii* strongly fluctuated in the range of 0–92% and 0–55%, respectively. *A. tepida* was relatively abundant in the middle-upper part of Section A (Capo San Marco), displaying peak occurrences of >50% between S25 and S31 (mudstones and muddy siltstones), whereas it was absent in the lower (between S1 and S12, marls) and upper parts of the section (Fig. 5). *A. beccarii* had a fluctuating pattern, achieving its highest frequency in S39 (55%, sandstones), but its relative abundance was low in the lowermost (from S1 to S11) and middle-upper parts of Section A (between S17 and S35), where it was replaced by *A. tepida*. In Section B between S36 and S47 consisting mainly of sandstones (Fig. 5), *A. beccarii* was the most frequent species. *H. germanica* and *E. macellum* showed a fluctuating pattern throughout the section with the highest relative abundances between S16

and S34, where the lithology consists of mudstones and muddy siltstones. *C. pseudoungerianus*, *M. pompilioides* and *Oridorsalis umbonatus* disappeared in the middle-upper part of Section A approximately from S20 (Fig. 5). *L. lobatula* showed a fluctuating pattern in section A with peaks ranging from 26-29% in marls (S1, S10) and a peak of 14% in mudstones (S4), while in Section B it only constituted 8-15% in four samples (S37-S39 and S43) consisting of mudstones and marls (Fig. 5). *Cibicidoides wuellerstorfi*, *H. boueana*, *Quinqueloculina seminula*, and *Cancris auriculus* had the highest relative abundance in the lower part of Section A between S1 and S18 (Fig. 5), then they disappeared (S21-S32) and re-occurred in Section B (S36 to S47). *E. crispum* had a peak in S34 (22%), S32 (21%) and S2 (14%) in Section A, while in Section B the relative abundance of this species ranged between 0% (S36, S39) and 42% (S40). *E. aculeatum* showed the highest relative abundance in the upper part of Section A (S29, S32, S34) in muddy siltstones and marls reaching 11%, and it was mostly absent in the middle part (S18-S26; Fig. 5). The *Bolivina* species mainly occurred in the lower part of Section A between S1 and S13, where the lithology consisted by mudstones and marls, whereas *B. echinata* reached its maximum relative abundance in S15 (27%) and disappeared in S25. *B. aculeata* was found in the lower part of Section A, where it reached the highest relative abundance in sample S7 with 33%, and in two samples of section B, S37 and S38.

In general, the relative abundances of almost all the species showed a decline in the middle-upper part of the succession, in correspondence with the increasing relative abundance of *A. tepida*.

4.2 Palaeodiversity indices and ecological groups

The palaeodiversity indices (S and H) displayed the similar trend (Fig. 6), with a marked decline in diversity between sample S18 and S31 (muddy siltstones and mudstones). In contrast, D was high in the middle-upper interval (Section A), due to the highest abundance of *A. tepida*. In the basal part of Section A, the diversity indices showed higher values than in the upper portion belonging to Section B (from S37 to S47; Fig. 6). In the Section A, S ranged from 4 to 28, whereas in the upper part of Section B (from S32 to S47), the number of species fluctuated between 7 and 14. In Section A (Fig. 6), H ranged between 0.4 and 2.9 and showed an increase in Section B, ranging from 1.6 to 2.0. The D had an opposite trend; the lowest values occurred in the lower part (Section A, from 0.1 to 0.3) and at the end of Section B (from

0.1 to 0.3), whereas in the middle part (Section A, between S18 to S31; Fig. 6), D reached 0.8. The FD values were lower in the lower part of Section A (from S1 to S8), and increased in the middle and upper part (between S9 and S32), with some exception (S15, S18, S19, S23; Fig. 6). After a peak in S36, a significant decrease in FD values occurred in the Section B.

Potential epiphytic species were abundant (about 78%) in the uppermost part of Section B (between S36 and S47; Fig. 6), whereas this group showed a fluctuating pattern in the lowermost part of Section A with peaks reaching 70% in some samples (S29, S32 and S34; Fig. 6). Nutrient-enriched conditions species were found abundant between S1 and S15 (up to 55%). Thereafter, this group declined in percentage in the middle-upper part of Section A and in Section B (about 3%; Fig. 6). Potential low salinity species occurred in the middle part of the succession, between S16 and S31 (Fig. 6) and they were lower in the Section A from S1 to SS15 and in the Section B (about 14%).

4.3 Multivariate analysis

The Q-mode Hierarchical Cluster Analysis grouped the samples into four separate clusters (A, B, C and D; Fig. 7) and two sub-clusters (C1 and C2). The main characteristics of the four clusters are set out in Table 2.

Cluster A (Fig. 7) encompasses 6 samples (S13, S18, S19, S21, S22, S24) all picked in the middle part of section A and characterized by fine-grained lithologies such as muddy siltstones and mudstones. *H. germanica* was the most frequent species with variable percentages between 53.0% and 67.4% (mean 59.2%) followed by *A. tepida* (1.0–27.0%, mean 19.2%) and other less abundant species: *E. macellum* (0–28.7%), *A. beccarii* (0–5.5%), *B. echinata* (0–2.6%). Species Richness ranges from 5 to 20, Shannon index from 0.8 to 1.6, whereas the dominance shows values between 0.3 and 0.5. The foraminiferal density varies between 69 and 853 specimens/5 cm^3 of dry sediment. Potential low salinity species represent the most frequent foraminifera (60.5–94.4%), followed by potential epiphytic species (1.5–34.2%) and nutrient-enriched conditions species (0–14.5%).

Cluster B (Fig. 7) includes 7 samples (S23, S27, S28, S29, S32, S34, S40) from the middle part of Section A (muddy siltstones and mudstones) and one sample from Section B (marls, S40). *E. macellum* characterizes the assemblage (23.6–61.9%, mean 44.5%). *E. crispum* (0–41.7%), *H. germanica* (0–

33.2%), *A. tepida* (0–21.5%), *E. aculeatum* (0–10.7%), and *Q. seminula* (0–7.1%) are also frequent (Table 2). Species Richness ranges from 4 to 14, H index from 1.0 to 1.9, whereas D showed values between 0.2 and 0.4. The foraminiferal density varies between 33 and 745 specimens/5 cm^3 of dry sediment. Potential epiphytic species (43.3–70.52%) characterized this cluster, whereas potential low salinity species are frequent ranging from 9.4% to 54.7%.

Cluster C can be subdivided in two sub-clusters (C1 and C2; Fig. 7). Sub-cluster C1 includes 8 samples, characterized by mudstones and sandstones: 7 belonging to Section B (S36, S37, S38, S39, S41, S43, S47) and one (S12) is part of Section A. *A. beccarii* is the most frequent species (23.7–54.9%, mean 36.8%) followed by *E. macellum* (0–23.9%, mean 12.3%), *E. crispum* (0–21.4%, mean 10.2%), *H. germanica* (5.2–20.8%, mean 12.3%), *L. lobatula* (0–14.8%, mean 5.6%), and *H. boueana* (0–12.7%, mean 3.7%). The Species Richness values ranges between 7 and 14, H from 1.5 to 2.1, with an average value of 1.8. The Dominance ranges from 0.2 to 0.3 and FD between 89 and 861 specimens/5 cm^3 of dry sediment. Potential epiphytic species dominates this sub-cluster (54–87.8%, mean 76.1%) followed by potential low salinity species (5.2–20.8%, mean 12.6%) and species indicating nutrient-enriched conditions (0–19.8%, mean 6.6%). Sub-cluster C2 groups 14 samples (S1-S11, S14, S15, S17) belonging to the lower part of Section A, characterized by fine-grained lithologies such as mudstones and marls: *B. aculeata* is the most frequent species with the variable percentages between 0 and 33.0% (mean 4.6%), followed by *H. germanica* (0–32.2%), *L. lobatula* (0–29.0%), and *B. echinata* (0–27.4%). Species Richness fluctuates from 14 to 28, H index from 1.9 to 2.9, whereas Dominance shows values between 0.1 and 0.2. The foraminiferal density varies between 131 and 760 specimens/5 cm^3 of dry sediment. Species adapted to live in organic matter enriched-conditions characterizes this sub-cluster, ranging from 22.6 to 54.8% (mean 42.6). Epiphytic species (15.7–46.3%, mean 33.3%) are common.

Cluster D includes 6 samples (S16, S20, S25, S26, S30, S31; Fig. 7) collected in the middle part of Section A and characterized by mudstones. *A. tepida* is the most frequent species ranging from 45.1% and 91.7% (mean 62.7%). *E. macellum* (2.4–33.0%), *A. beccarii* (0–25.0%) and *H. germanica* (0–20.9%), are other common species of this cluster. Species Richness ranges from 4 to 18, H from 0.4 to 1.8, whereas the Dominance shows highest values between 0.3 and 0.8 (on the average 0.5). The foraminiferal density varies between 443 and 723 specimens/5 cm^3 of dry sediment (mean 608). The

analysis of ecological groups reveals a dominance of hypohaline species (45.1–92.7%, mean 70.1%; Table 2).

In PCA, 33.6% of the data variance can be explained by the first two principal components (Fig. 8A), and 31.0% of it by the first and third principal components (Fig. 8B). The eigenvalues of components 1, 2 and 3 are 5.0, 2.7 and 2.1 respectively (Fig. 8C). The percentages of *B. arta*, *B. dilatata*, *C. pseudoungerianus*, *M. pompilioides*, *L. lobatula* and *E. macellum* are the predominant elements in the first component, while the major contributions in the second component are from *C. auriculus*, *C. wuellerstorfi*, *B. dilatata*, and *Nonion fabum*, in the third component the predominant elements are *A. beccarii*, *E. crispum*, *H. germanica*, and *N. fabum*.

PCA analysis placed the stations in approximately the same groups as obtained with Q mode cluster analysis. Accordingly, those samples on the right part of the diagram (Figs 8A and B), belonging to Sub-cluster C2 (except S12; Fig. 8A) are characterized by the presence of *B. arta*, *B. dilatata*, *C. pseudoungerianus*, *C. wuellerstorfi*, *C. auriculus*, *L. lobatula*, *M. pompilioides*, *H. boueana*, *B. echinata*, those on the left-bottom part (Clusters A, B and D) by *A. tepida*, *E. macellum* and *H. germanica* (Figs 8A and B), whereas those on the left-upper part (Sub-cluster C1) by *E. crispum*, *E. aculeatum*, *Textularia agglutinans* and *A. beccarii* (Fig. 8A).

5. Discussion

5.1 Palaeoecological intervals

The benthic foraminiferal analysis carried out on sections A and B (Capo San Marco and Monte Palla; Fig. 1) produced a palaeoecological framework of this marginal basin during the Messinian. The studied record covers the pre-MSC interval (7.251–5.97 Ma) to the onset of the MSC (stage 1, 5.97–5.6 Ma) up to the Messinian Erosional Surface (MES) recorded in stage 2 (5.6–5.55 Ma) (*sensu* Roveri et al., 2014). The palaeoecological conditions have been compared to planktonic bioevents and the content of the macrofaunal proxies.

The environmental evolution in the pre-MSC interval is characterized by a progressive shallowing trend, starting with the upper bathyal-circalittoral zone and evolving towards restricted conditions (Capo San Marco Formation - CSMF), as documented by benthic foraminiferal microfaunas. Also, the absence of planktonic foraminifera in the middle-upper part of the pre-MSC interval (CSMF) could be related to hypohaline conditions (lagoonal and brackish environments). In the upper part of M. Palla section (Torre del Sevo Formation - TSF; Fig. 1), clearly marine species indicate that this marginal basin was not desiccated and was connected with the open sea. In the Sinis Laminated Limestone Formation (SLLF; Fig. 1), planktonic and benthic species completely disappear, probably as a consequence of the true MSC onset. The benthic foraminiferal analyses allowed us to recognize three palaeoecological intervals (A-B-C; Fig. 9), which are characterized by different palaeobiocoenosis. In this paper, the A and B intervals have been interpreted as belonging to the pre-MSC interval, whereas C refers to stage 1 of the MSC (*sensu* Roveri et al., 2014).

Interval A includes samples from S1 to S15 (Fig. 1) that correspond to the lowermost part of the CSMF are mainly grouped on the right side of the PCA (Fig. 8A, B). In its lowermost portion, Interval A starts with a remarkable microbial-bryozoan mound that is contained in muddy-silty sediment characterized by a poor benthic foraminiferal assemblage (sample S1). Successively (samples S2-S15; Fig. 1), micropalaeontological data revealed the occurrence of a rich foraminiferal assemblage, which is also expressed by diversity indices (S and H; Fig. 6). The interval A includes samples belonging to Sub-cluster C2 (Fig. 7). Interval A reveals a simultaneous presence of epi- and shallow to intermediate infaunal species, relatively high diversity and relative high abundance of opportunistic species. Consequently, the interval could be interpreted as being the result of the accumulation of sediment in a vegetated open marine ecosystem (upper bathyal/circalittoral evolving to infralittoral), with mesotrophic to eutrophic conditions and degraded organic matter at the sea bottom. The benthic foraminifera assemblages appear represented by species with a wide depth range from circalittoral to deep water like *B. aculeata*, *B. echinata*, *C. pseudoungerianus*, *C. wuellerstorfi*, *M. pompilioides*, *O. umbonatus* (see Appendix A for ecological information). The depth distribution of *M. pompilioides* is of particular interest because in modern ecosystems along the Atlantic coast, this species is reported as a clearly deep

water indicator (2000 m and beyond) that seems to prefer a high oxygen content (e.g., Mojtahid et al., 2010; Jorissen et al., 1998; Schmiedl et al., 1997; Sjoerdsma and Van der Zwaan, 1992) whereas in the Mediterranean region, this species was also found in circalittoral zone where it is tolerant to poorly oxygenated and nutrient-rich environments (e.g., Bergamin et al., 1997; Frezza et al., 2005; Frezza and Carboni, 2009). The relatively high percentage of bolivinids and buliminids indicates mesotrophic to eutrophic conditions and degraded organic matter at the sea bottom (e.g., Van der Zwaan, 1982; Jorissen et al., 1992; Violanti, 1996; Mojtahid et al., 2009). Moreover, according to Hemleben et al. (1989) and Sierro et al. (2003), *Globigerina bulloides*, *Turborotalita quinqueloba* and the Neogloboquadrinids, proliferate today in cold, nutrient-rich waters. Their simultaneous presence in interval A (Fig. 5) could be suggest the existence of eutrophic conditions and normal salinity in the surface water. Shallow-water species, mainly epiphytic of infralittoral-circalittoral zones (*L. lobatula, H. boueana, E. macellum*, *E. crispum*) also occur, reaching the highest abundance (about 54%) in sample S12 (Fig. 6). In spite of the fluctuating presence of deep-water species (*C. pseudoungerianus, C. wuellerstorfi, M. pompilioides, O. umbonatus,* bolivinids and buliminids), the low values of P/B ratio and the continuous upward increase of the relative abundance of shallow-water species, mainly *A. beccarii*, *H. boueana* and *H. germanica* suggests a progressively shallowing environment (infralittoral) from sample S8 to S14 (Fig. 1). Currently, *A. beccarii*, *E. macellum, L. lobatula*, *H. boueana,* and *E. crispum* are widespread Mediterranean species that live prevalently on sandy or sandy-mud infralittoral/circalittoral bottoms, well-oxygenated environment with a vegetation meadow present in areas nearby (e.g., Jorissen, 1987; Langer, 1993; Sgarrella and Moncharmont Zei, 1993; Milker et al., 2009; Buosi et al., 2012; 2013a). Also, planktonic foraminifera become less abundant after the peak recognized at about 3.0 m (sample S6; Fig. 4) and completely disappear at about 7.5 m (sample S15; Fig. 4), whereas calcareous nannoplankton shows a decline in species richness leading to rather poor and monotonous assemblage in the upper part of this interval (from S8; Fig. 4) that seems to indicate restricted environmental conditions. Thus, a progressive shallowing from the upper bathyal/circalittoral to the infralittoral can be reconstructed in this interval.

Interval B (between samples S16 and S34; Fig. 1) is interpreted as a phase of sediment accumulation in lagoons and/or brackish environments. These samples are grouped together on the right side of the PCA (Fig. 8A, B). This interval includes several mudstone layers alternated with muddy siltstone in the middle part of the CSMF. The macrofaunas is mostly represented by bivalves, such as *C. gibba*, *Abra alba* and *Macoma elliptica*. The benthic foraminiferal data show a significant decrease in the palaeodiversity indices (S, H, and FD). The dominance of potential low salinity foraminiferal species (*A. tepida*, *H. germanica*, Fig. 5), low relative abundances of miliolids and the absence of planktonic species (Arnold and Parker, 1999; Retailleau et al., 2009) suggest hypohaline conditions. Furthermore, *A. tepida* is a euryhaline cosmopolitan species that mainly lives in lagoons and shallow-normal to shallow-brackish marine marginal environments, which are characterized by lower salinity and is also known for its great tolerance of stressed conditions (e.g., Jorissen, 1988; Debenay et al., 1998; Debenay, 2000; Ruiz et al., 2007; Frezza and Carboni, 2009; Buosi et al., 2013b; Goineau et al., 2015; Salvi et al., 2015). In restricted environments, its distribution is related to the prevailing sea-to-freshwater gradient (Debenay and Guillou, 2002). *H. germanica* and *E. macellum* were found associated with phytal substrate in modern Mediterranean infralittoral zones (e.g., Langer 1993; Frezza and Carboni, 2009; Mateu-Vicens et al., 2014; Benedetti and Frezza, 2016). The presence of bivalves, such as *C. gibba*, *A. alba* and *M. elliptica* also suggests a lagoon environment with a low salinity before the deposition of the Terminal Carbonate Complex (TCC). These bivalve species are found within a large range of water depths. Their optimal habitat is however approximately 20-40 m, in estuarine and near coastal areas characterized by muddy sediments (Van Hoey et al. 2005; Degraer et al., 2006; Holmes and Miller, 2006; Hrs-Brenko, 2006). *C. gibba* is in particular extremely well adapted to living in hypohaline conditions due to its high tolerance of variable salinity (e.g., Holmes and Miller, 2006; Zettler et al., 2013). In addition, Cherchi et al. (1978) reported the presence of coal fragments and undeterminable plant remains (marsh-vegetation) that can be considered further elements supporting the presence of a shallow hypohaline lagoon.

Interval C includes samples from the sedimentary succession of the Monte Palla section (between samples S36 and S50, Sub-cluster C1) belonging to the TSF, which is deposited unconformably above

the laminated limestone (SLLF; Fig. 1) barren in micro- and macrofossils. This interval groups samples that are mainly located on the upper-left side of the PCA (Fig. 8A, B). The lower part of the TSF consists of marine siliciclastic deposits bearing macrofaunas (pectinids). These alternate with sandy marls, which are sometimes rich in disarticulated, chaotically-arranged remains of bivalves (*Chama gryphoides*, *Coralliophaga lithophagella*), balanids, vermetids, echinoids and benthic foraminifera indicating high-energy environment. In the upper part of the TSF (Fig. 1), euryhaline short marine episodes, intercalated in siliciclastic deposits, are indicated by the occurrence of bivalves, gastropods, and benthic and rare planktonic foraminifera (*G. bulloides*, *Orbulina universa*). The benthic foraminiferal assemblage is dominated by marine species that are usually related to normal salinity conditions and vegetated sea-bottom (*A. beccarii*, *H. germanica*, *E. crispum*, *E. macellum* and *L. lobatula*). The major difference with Interval A is due to the clear absence of opportunistic infaunal species like bolivinids and buliminids and low values of Foraminiferal Density (FD). The C interval probably indicates the re-establishment of normal salinity marine conditions and the development of marine vegetation on the sea bottom, which is also recognized by the increase in the palaeodiversity indices and the presence of epiphytic and epifaunal species.

5.2 Comparison with other marginal basins

The micropalaeontological content from the marginal basin of the Sinis allows us to provide significant information on the palaeoecological changes related to the MSC. In the Sinis Basin, the palaeoenvironmental conditions, which show a progressive shallowing trend and are affected by salinity fluctuations, have been intermittently favourable to the life of marine biotas, similar to some eastern Spanish marginal basins (e.g., Sorbas, Vera and Almeria; Braga et al., 1995; Riding et al., 1998; Goubert et al., 2001; Corbí et al., 2016).

Marine conditions (upper bathyal/circalittoral to infralittoral) with mesotrophic to eutrophic conditions and degraded organic matter at the sea bottom (palaeoecological Interval A), are found in the lower part of the CSMF (Fig. 9) as shown by macro- and microfaunas (Cherchi et al., 1978; Moissette et al., 2002; André et al., 2004; Saint Martin, 2010). Similar palaeoenvironmental conditions have been documented in the pre-evaporitic Abad Member of Sorbas Basin (between 7.2 and 5.96 Ma; Goubert et al., 2001),

where the upper part of the pre-evaporitic unit (Abad Member) corresponds to a distal platform (upper bathyal to circalittoral) mainly characterized by infaunal genus (*Bulimina*, *Uvigerina*, *Rectuvigerina* and *Brizalina*).

According to several studies, a deep-water stagnation associated to a high supply of organic matter and a significant decrease in the oxygen content occurred in Sicily (Bellanca et al. 2001; Blanc-Valleron et al. 2002); North (M. del Casino) and central Italy (Trave section; Iaccarino et al., 2008; Di Stefano et al., 2010); NE Crete (Faneromeni; Kouwenhoven et al., 2003), and Cyprus (Kouwenhoven et al., 2006), between 7.02 and 6.70 Ma. In the Sinis Basin, levels rich in radiolarians and diatoms in the pre-MSC claystones-mudstones of the CSMF, deposited of the microbial mound, could indicate isolation and water stratification (Rouchy, 1980) and/or changes in nutrient content of surface waters (Martin and Braga, 1994; Sierro et al., 1997). The deposition of laminated diatomaceous marls is recorded in several pre-evaporitic deposits from Gavdos Island (Drinia et al., 2007) and Sicily (Bellanca et al., 2001; Blanc-Valleron et al., 2002), and it is considered an additional event associated with the restriction in the Mediterranean–Atlantic exchanges and the reduction of the deep-water ventilation.

In our record, a shallowing trend is also shown by the transition from open marine conditions (interval A) to lagoonal facies (interval B). In interval B, salinity fluctuations are highlighted by a barren planktonic zone in the mid-upper part of the CSMF and by the increasing presence of species indicating potentially low salinity conditions like *A. tepida* and *H. germanica* and a relative low abundance of miliolids (Figs. 5 and 6). The last group of benthic foraminifera inhabiting the sea floor disappears just before the deposition of the unfossiliferous SLLF (Fig. 1; Cherchi et al. 1978, 1985; Cornée et al., 2008). Considering that in the marginal basins, the MSC onset is marked by the deposition of the lowermost gypsum bed at ~5.97 Ma (Manzi et al., 2013; Roveri et al., 2014) in water depths shallower than 200 m and no primary gypsum deposit outcrops onshore in the Sinis area, we hypothesize that the onset of the MSC in the examined section could be placed at the level that coincide with the complete and sustained disappearance of planktonic and benthic assemblages (barren zone; Fig. 9) that correspond to the SLLF formation. Offshore in the Sinis Basin, the seismic survey shows a thick evaporitic layer, which is truncated by the polyphasic erosion surface (MES; Geletti et al., 2014).

A complex sedimentological architecture, with the development of a siliciclastic-carbonate platform, characterizes the upper part of the Messinian succession in the Sinis basin. This mixed platform shows aggradation and progradation phases, interrupted by subaerial exposures and erosional surfaces that could be relative to sea level fluctuations. The late Messinian carbonate deposits are grouped into the common definition of the "Terminal Carbonate Complex" (TCC). The age of the TCC is controversial (Roveri et al., 2014), but it could be coeval with the deposition of the primary evaporites and therefore may record the MSC onset (Cunningham et al., 1994; Cornée et al., 2006) and/or the entire duration of the MSC (Roveri et al., 2009).

In the Sinis area, the TCC is composed of two units, the SLLF and the TSF (Fig. 1), which are separated by a subaerial erosional surface. A siliciclastic-carbonate system with marine fossiliferous levels and increases of fluvial inputs characterizes the TSF, whereas the SLLF consists of unfossiliferous cyclic-laminated limestones. Due to the presence of subaerial erosional surfaces and the unconformity contact between the upper part of CSMF and SLLF and between SLLF and TSF, a stratigraphic hiatus can be hypothesized. We cannot exclude that during subaerial conditions gypsum level may have been eroded. The TSF above shows several marine litho-biofacies, including oolitic grainstones, microbial stromatolitic beds, vermetid and balanid fragments, very rare rhodolithids and hermatypic corals. In the TCC of the Sinis Basin, the stressed environment is emphasized by the extreme scarcity of chlorozoan facies (*Halimeda*) and of scleractinian corals. The presence of microbialite-dominated facies is common in the TCC of many western Mediterranean basins during the late Messinian (e.g., Riding et al., 1998; Braga et al., 2006; Saint Martin, 2010). The progressive decrease in the diversity of the reef builders and the increase of microbial activity are related to highly-stressed conditions linked to the reduction of the Atlantic-Mediterranean connection (Roveri et al., 2009).

During the deposition of the TSF (Fig. 1), the ecological conditions were intermittently favourable to the life of foraminiferal assemblages and macrofaunas. The foraminiferal species occurring in the middle part of this formation belong to marine infralittoral benthic group (*A. beccarii*, *E. crispum*, *E. macellum*, *L. lobatula*) and rare small globigerinids. The presence of these species is related to an upper Messinian reflooding before the uppermost terminal carbonates (Bache et al., 2012; Pérez-Asensio et al., 2013). The occurrence of foraminiferal species in the TSF supports the idea of a limited impact on

the fauna living in the infralittoral environment during the MSC in the Sinis Basin. This is in agreement with the findings of other studies (e.g., Riding et al., 1998; Goubert et al., 2001), and shows that several marginal basins (for example, the Los Yesos area in Sorbas Basin; Goubert et al., 2001) during the salinity crisis were not continuously desiccated.

In the Sinis Basin, the TCC is abruptly cut by a strong subaerial erosion (MES). This could have lasted from 5.77 to 5.3 Ma (Cornée et al., 2008), in comparison with the radiometric data from the Melilla-Nador Basin (Morocco). Offshore, in the western margin of Sardinia, the MES was identified at the top of the Messinian sequence (Cornée et al., 2008). According to Geletti et al. (2014), seismic evidence shows that the MES is present across the middle and upper slopes of the western Sardinian margin, and can be recognized down to the lower slope, where it interfingers with the evaporites, which thicken basin-wards.

6. Conclusions

The quantitative analyses of benthic foraminiferal assemblages from the Messinian succession of the Sinis area allow us to investigate the palaeoenvironmental changes that took place during the pre-Messinian Salinity Crisis and MSC intervals.

The marginal Sinis Basin is characterized by upper bathyal/circalittoral conditions, evolving into sublittoral/infralittoral-lagoonal settings during the pre-MSC interval. In the lower part of the Capo San Marco Formation, the palaeoenvironmental condition was quite favourable for benthic foraminiferal life, as highlighted by epiphytic-epifaunal species (e.g., elphidiids, *L. lobatula, A. beccarii, H. boueana; Melonis* spp.) and locally opportunistic species (bolivinids and buliminids). The presence of opportunistic species appears also to be related to mesotrophic to eutrophic conditions and degraded organic matter at the sea bottom. At the end of the pre-MSC phase, the Sinis Basin evolved gradually into a sublittoral-infralittoral environment followed by a hypohaline lagoon, as suggested by *A. tepida, H. germanica* and *E. macellum*. The planktonic and benthic barren zone in the SLLF indicates an interval of a severe biological crisis probably related to MSC onset.

The last deposits of the Sinis Basin consist of two depositional units (SLLF and TSF) ascribed to the TCC and separated by subaerial erosion. In the upper part of the TSF, the temporary re-establishment of euryhaline sub-littoral conditions is documented by macrofaunas, ostracods, benthic foraminifera (elphidiids, miliolids) and rare planktonic species (*G. bulloides*, *O. universa*). The presence of rapid reflooding episodes during the MSC stage (Torre del Sevo Formation) indicates that the marginal Sinis Basin was not permanently desiccated, in agreement with other marginal Spanish basins.

A strong and wide erosional phase, attributed to the MES, cut the Messinian succession of the Sinis Basin before the Zanclean flooding event.

Acknowledgements

The authors are grateful to A. Russo (Modena University) and G. Salvi (Trieste University) for their scientific support. We are also grateful to BTek Services Ltd. (Buxton, United Kingdom) for English language improvement. The authors warmly thank the reviewers, the editor and F. Jorissen for their useful comments and suggestions, which greatly improved the manuscript.

Funding: This research did not receive any specific grant from funding agencies in the public, commercial, or not-for-profit sectors.

References

Aguirre, J., Sánchez-Almazo, I.M., 2004. The Messinian post-evaporitic deposits of the Gafares area (Almería–Níjar basin, SE Spain). A new view of the “Lago-Mare” facies. Sedimentary Geology 168, 71–95.

André, J.P., Saint Martin, J.P., Moissette, P., Garcia, F., Cornée, J.J., Ferrandini, M., 2004. An unusual Messinian succession in the Sinis Peninsula, western Sardinia, Italy. Sediment. Geol. 167, 41–55.

Arnold, A.J., Parker, W.C., 1999. Biogeography of planktonic foraminifera. In: Modern Foraminifera, edited by: Sen Gupta, B., Kluwer Academic Publishers, Dordrecht, the Netherlands, 103–122.

Bache, F., Gargani, J., Suc, J.-P., Gorini, C., Rabineau, M., Popescu, S.-M., Leroux, E., Couto, D.D., Jouannic, G., Rubino, J.-L., Olivet, J.-L., Clauzon, G., Dos Reis, A.T., Aslanian, D., 2015. Messinian evaporite deposition during sea level rise in the Gulf of Lions (Western Mediterranean). Marine and Petroleum Geology 66, 262-277.

Bache, F., Popescu, S.-M., Rabineau, M., Gorini, C., Suc, J.-P., Clauzon, G., Olivet, J.-L., Rubino, J.-L., Melinte-Dobrinescu, M.C., Estrada, F., Londeix, L., Armijo, R., Meyer, B., Jolivet, L., Jouannic, G., Leroux, E., Aslanian, D., Dos Reis, A.T., Mocochain, L., Dumurdzanov, N., Zagorchev, I., Lesic, V., Tomic, D., Cagatay, M.N., Brun, J.-P., Sokoutis, D., Csato, I., Ucarkus, G., Cakir, Z., 2012. A two-step process for the reflooding of the Mediterranean after the Messinian Salinity Crisis. Basin Research 24 (2), 125–153.

Bellanca, A., Caruso, A., Ferruzza, G., Neri, R., Rouchy, J.M., Sprovieri, M., Blanc-Valleron, M.M., 2001. Transition frommarine to hypersaline conditions in theMessinian Tripoli Formation from the marginal areas of the central Sicilian basin. Sedimentary Geology 140 (1–2), 87–105.

Benedetti, A., Frezza, V., 2016. Benthic foraminiferal assemblages from shallow-water environments of northeastern Sardinia (Italy, Mediterranean Sea). Facies 62: 14. doi:10.1007/s10347-016-0465-9

Bergamin, L., Carboni, M.G., di Bella, L., 1997. *Melonis pompilioides* (Fichtel & Moll) and *Melonis barleeanus* (Williamson) from Pliocene, Pleistocene and Holocene sediments of central Italy. Geologica Romana 33, 29–45.

Blanc-Valleron, M.-M., Pierre, C., Caulet, J.P., Caruso, A., Rouchy, J.M., Cespuglio, G., Sprovieri, R., Pestrea, S., Di Stefano, E., 2002. Sedimentary, stable isotope and micropaleontological records of palaeoceanographic change in the Messinian Tripoli Formation (Sicily, Italy). Palaeogeography, Palaeoclimatology, Palaeoecology 185, 255–286.

Braga, J.C., Martín, J.M., Riding, R., 1995. Controls on microbial dome fabric development along a carbonate-siliciclastic shelf-basin transect, Miocene, SE Spain. Palaios 10, 347–361.

Braga, J.C., Martín, J.M., Riding, R., Aguirre, J., Sanchez-Almazo, I.M., Dinares-Turell, J., 2006. Testing models for the Messinian salinity crisis: the Messinian record in Almería, SE Spain. Sedimentary Geology 188–189, 131–154.

Buosi, C., Armynot Du Châtelet, E., Cherchi, A., 2012. Benthic foraminiferal assemblages in the current-dominated Strait of Bonifacio (Mediterranean Sea). J. Foramin. Res. 42 (1): 39–55.

Buosi, C., Cherchi, A., Ibba, A., Marras, B., Marrucci, A., Schintu, M., 2013a. Preliminary data on benthic foraminiferal assemblages and sedimentological characterisation from some polluted and unpolluted coastal areas of Sardinia (Italy). Bollettino della Società Paleontologica Italiana 52, 35–44. doi: 10.4435/BSPI.2013.08

Buosi, C., Cherchi, A., Ibba, A., Marras, B., Marrucci, A., Schintu, M., 2013b. Benthic foraminiferal assemblages and sedimentological characterisation of the coastal system of the Cagliari area (Southern Sardinia, Italy). Bollettino della Società Paleontologica Italiana 52, 1–9. doi:10.4435/BSPI.2013.04

Caruso, A., Pierre, C., Blanc-Valleron, M.-M., Rouchy, J.M., 2015. Carbonate deposition and diagenesis in evaporitic environments: The evaporative and sulphur-bearing limestones during the settlement of the Messinian Salinity Crisis in Sicily and Calabria. Palaeogeography, Palaeoclimatology, Palaeoecology 429, 136–162.

Casula, G., Cherchi, A., Montadert, L., Murru, M., Saria, E., 2001. The Cenozoic graben system of Sardinia (Italy): geodynamic evolution from new seismic and field data. Mar. Pet. Geol. 18, 863–888.

Cherchi, A., 1974. Appunti biostratigrafici sul Miocene della Sardegna (Italia). Inter. Néogéne Medit., Lyon-1971, Mem. B.R.G.M., 78: 433-445, Lyon.

Cherchi, A., Martini, E., 1981. Calcareous nannoplankton and planktonic foraminifera of the Messinian and basal Pliocene from Capo San Marco (W. Sardinia). Géol. Méditerr. 7, 109–119.

Cherchi, A., Montadert, L., 1982. Oligo - Miocene rift of Sardinia and the early history of the Western Mediterranean Basin. Nature 298, 736–739.

Cherchi, A., Tremolieres, P., 1984. (New data on the structural evolution of the Mesozoic-Cenozoic of Sardinia and its geodynamic implications for the Mediterranean region). Comptes Rendus - Academie des Sciences, Serie II 298(20), 889–894.

Cherchi, A., D'Onofrio, S., Martini, E., Murru, M., Robba, E., Russo, A., 1985. Messinian of Capo S. Marco section. In: Cherchi, A. (Ed.), Guidebook 19th European Micropaleontological Colloquium, Sardinia, Agip, Cagliari, pp. 290-301.

Cherchi, A., Marini, A., Murru, M., Robba, E., 1978. Stratigrafia e paleoecologia del Miocene superiore della penisola del Sinis (Sardegna occidentale). Riv. Ital. Paleont. Strat. 9, 773–1036.

Cimerman, F., Langer, M.R., 1991. Mediterranean Foraminifera. Slovenska Akademija Znanosti in Umetnosti. Academia Scientiarum et Artium Slovenica Cl. 4 Historia Naturalis, 30, Ljubljana (93pp).

Corbí, H., Soria, J.M., Lancis, C., Giannetti, A., Tent-Manclús, J.E., Dinarès-Turell, J., 2016. Sedimentological and paleoenvironmental scenario before, during, and after the Messinian Salinity Crisis: The San Miguel de Salinas composite section (western Mediterranean). Marine Geology 379, 246–266.

Cornée, J.J., Ferrandini, M., Saint Martin, J.-P., Münch, Ph., Moullade, M., Ribaud-Laurenti, A., Saint Martin, S., Roger, S., Ferrandini, J., 2006. The Late Messinian erosional surface and the subsequent reflooding in the Mediterranean: new insights from the Melilla–Nador basin (Morocco). Palaeogeogr. Palaeoclimatol. Palaeoecol. 230, 129–154.

Cornée, J.J., Maillard, A., Garcia, F., Conesa, G., Saint Martin, J.P., Sage, F., Münch, P., 2008. Field-evidence for the late Messinian erosional surface in the Sinis peninsula, western Sardinia, Italy. Sediment. Geol. 210, 48–60.

Cunningham, K.J., Farr, M.R., Rakic-El Bied, K., 1994. Magnetostratigraphic dating of an Upper Miocene shallow-marine and continental sedimentary succession in northeastern Morocco. Earth and Planetary Science Letters 127, 77–93.

Debenay, J.-P., 2000. Foraminifers of paralic tropical environments. Micropaleontology 46, 153–160.

Debenay, J.P., 2012. A guide to 1,000 Foraminifera from southwestern Pacific New Caledonia. IRD Éditions.

Debenay J.-P., Guillou J.-J., 2002. Ecological transitions indicated by foraminiferal assemblages in paralic environments. Estuaries 25, 1107–1120.

Debenay, J.-P., Bénéteau, E., Zhang, J., Stouff ,V., Geslin, E., Redois, F., Fernandez-Gonzalez, M., 1998. *Ammonia beccarii* and *Ammonia tepida* (Foraminifera): morphofunctional arguments for their distinction. Mar. Micropaleontol. 34, 235–244.

Degraer, S., Wittoeck, J., Appeltans, W., Cooreman, K., Deprez, T., Hillewaert, H., Hostens, K., Mees, J., Vanden Berghe, E., Vincx, M., 2006. The macrobenthos atlas of the Belgian part of the North Sea. Belgian Science Policy, Brussel. ISBN 90-810081-6-1.

Di Stefano, A., Verducci, M:, Lirer, F., Ferraro, L., Iaccarino, S.M., Hüsing, S.K., Hilgen, F.J., 2010. Paleoenvironmental conditions preceding the Messinian Salinity Crisis in the Central Mediterranean: Integrated data from the Upper Miocene Trave section (Italy). Palaeogeogr. Palaeoclimatol. Palaeoecol. 297, 37–53.

Drinia, H., Antonarakou, A., Tsaparas, N., Kontakiotis, G., 2007. Palaeoenvironmental conditions preceding the Messinian Salinity Crisis: a case study from Gavdros Island. Geobios 40, 251–265.

Duncan, R., Ginesu, S., Secchi, F., Sias, S., 2011. The recent evolution of the Sinis region (western coast of Sardinia, Italy) on the basis of new radiometric data of the Pliocene volcanism. Geogr. Fis. Dinam. Quat. 14, 175–181.

Esteban, M., 1979. Significance of the Upper Miocene coral reefs of the western Mediterranean. Palaeogeography, Palaeoclimatology, Palaeoecology 29, 169–188.

Flecker, R., Krijgsman, W., Capella, W., de Castro Martíns, C., Dmitrieva, E., Mayser, J.P., Marzocchi, A., Modestu, S., Ochoa, D., Simon, D., Tulbure, M., van den Berg, B., van der Schee, M., de Lange, G., Ellam, R., Govers, R., Gutjahr, M., Hilgen, F., Kouwenhoven, T., Lofi, J., Meijer, P., Sierro, F.J., Bachiri, N., Barhoun, N., Chakor Alami, A., Chacon, B., Flores, J.A., Gregory, J., Howard, J., Lunt, D., Ochoa, M., Pancost, R., Vincent, S., Zakaria Yous, M., 2015. Evolution of the Late Miocene Mediterranean–Atlantic gateways and their impact on regional and global environmental change. Earth-Science Reviews 150, 365–392. DOI: 10.1016/j.earscirev.2015.08.007

Frezza, V., Carboni, M.G., 2009. Distribution of recent foraminiferal assemblages near the Ombrone River mouth (Northern Tyrrhenian Sea, Italy). Revue de Micropaléontologie: 52, 43-66.

Frezza, V., Carboni, M.G., Matteucci, R. 2005. Recent foraminiferal assemblages near Ponza Island (Central Tyrrhenian Sea, Italy). Bollettino della Società Paleontologica Italiana 44, 155-173.

Geletti, R., Zgur, F., Del Ben, A., Buriola, F., Fais, S., Fedi, M., Forte, E., Mocnik, A., Paoletti, V., Pipan, M., Ramella, R., Romeo, R., Romi, A., 2014. The Messinian Salinity Crisis: New seismic evidence in the West-Sardinian Margin and Eastern Sardo-Provençal basin (West Mediterranean Sea). Mar. Geol. 351, 76–90.

Gennari, R., Manzi, V., Angeletti, L., Bertini, A., Biffi, U., Ceregato, A., Faranda, C., Gliozzi, E., Lugli, S., Menichetti, E., Rosso, A., Roveri, M., Taviani, M., 2013. A shallow water record of the onset of the Messinian salinity crisis in the Adriatic foredeep (Legnagnone section, Northern Apennines). Palaeogeogr. Palaeoclimatol. Palaeoecol. 386, 145–164.

Goineau, A., Fontanier, C., Mojtahid, M., Fanget, A.-S., Bassetti, M.-A., Berné, S., Jorissen, F.J., 2015. Live–dead comparison of benthic foraminiferal faunas from the Rhône prodelta (Gulf of Lions, NW Mediterranean): Development of a proxy for palaeoenvironmental reconstructions. Marine Micropaleontology 119, 17–33.

Gorini, C., Montadert, L., Rabineau, M., 2015. New imaging of the salinity crisis: Dual Messinian lowstand megasequences recorded in the deep basin of both the eastern and western Mediterranean. Marine and Petroleum Geology, 66, 278-294.

Goubert, E., Néraudeau, D., Rouchy, J.M., Lacour, D., 2001. Foraminiferal record of environmental changes: Messinian of the Los Yesos area (Sorbas Basin, SE Spain). Palaeogeogr. Palaeoclimatol. Palaeoecol. 175, 61–78.

Hammer, Ø., Harper, D.A.T., Ryan, P.D., 2001. PAST: Paleontological statistics software package for education and data analysis. Palaeontologia Electronica, 4(1), 9pp., <http://www.palaeoelectronica.org>.

Hemleben, C., Spindler, M., Anderson, O.R., 1989. Modern Planktonic Foraminifera. Springer, New York, pp. 1–363.

Hilgen, F.J., Bissoli, L., Iaccarino, S., Krijgsman, W., Meijer, R., Negri, A., Villa, G., 2000a. Integrated stratigraphy and astrochronology of the Messinian GSSP at Oued Akrech (Atlantic Morocco). Earth Planet. Sc. Lett. 182, 237–251.

Hilgen, F.J., Iaccarino, S., Krijgsman, W., Langereis, C.G., Villa, G., Zachariasse, W.J., 2000b. The global boundary stratotype section and point (GSSP) of the Messinian Stage (uppermost Miocene). Episodes 23, 172–178.

Hilgen, F.J., Kuiper, K., Krijgsman,W., Snel, E., van der Laan, E., 2007. Astronomical tuning as the basis for high resolution chronostratigraphy: the intricate history of the Messinian Salinity Crisis. Stratigraphy 4, 231–238.

Holmes, S.P., Miller, N., 2006. Aspects of the ecology and population genetics of the bivalve *Corbula gibba*. Mar. Ecol. Prog. Ser. 315, 129–140.

Hottinger, L., Halicz, E., Reiss, Z., 1993. Recent Foraminiferida from the Gulf of Aqaba, Red Sea. Academia Scientiarum et Artium Slovenica, Classis IV: Historia Naturalis, 33, Lubljana (179pp).

Hrs-Brenko, M., 2006. The basket shell, *Corbula gibba* Olivi, 1792 (Bivalve Mollusks) as a species resistant to environmental disturbances: A review. Acta Adriatica 47, 49–64.

Hsü, K.J., 1972. Origin of Saline Giants: a critical review after the discovery of the Mediterranean evaporite. Earth-Science Reviews 8, 371–396.

Hsü, K.J., 1973. The desiccated deep-basin model for the Messinian events. In: Drooger, C.W. (Ed.), Messinian Events in the Mediterranean. North-Holland Publ. Co., Amsterdam, pp. 60–67.

Hsü, K., Ryan,W.B.F., Cita, M., 1973a. Late Miocene desiccation of the Mediterranean. Nature 242, 240.

Hsü, K.J., Cita, M.B., Ryan, W.B.F., 1973b. The origin of the Mediterranean evaporites. In: Ryan,W.B.F., Hsü, K.J., Cita, M.B. (Eds.), Initial Reports of the Deep Sea Drilling Project 13, Part 2. U.S. Government Printing Office, Washington D.C., pp. 1203–1231.

Iaccarino, S.M., 1985. Mediterranean Miocene and Pliocene planktic foraminifera. In Bolli H.M., Saunders J.8., Perch-Nielsen K., pp. 283-31,4, Cambridge University Press.

Iaccarino, S.M., Bertini, A., Di Stefano, A., Ferraro, L., Gennari, R., Grossi, F., Lirer, F., Manzi, V., Menichetti, E., Ricci Lucchi, M., Taviani, M., Sturiale, G., Angeletti, L., 2008. The Trave section (Monte dei Corvi, Ancona, Central Italy): an integrated paleontological study of the Messinian deposits. Stratigraphy 5, 281–306.

Iaccarino, S.M., Premoli, S.I., Biolz, M., Foresi, L.M., Lirer, F., Urco, E., and Petrizzo, M.R., 2007, Practical Manual of Neogene Planktonic Foraminifera: VI Course (February 19–23): Neogene: Perugia, Italy, International School on Planktonic Foraminifera, 181 p.

Jorissen, F.J., 1987. The distribution of benthic foraminifera in the Adriatic Sea. Marine Micropaleontology 12, 21-48.

Jorissen F.J., 1988. Benthic foraminifera from the Adriatic Sea: priniciples of phenotypic variation. Utrecht Micropaleontological Bulletins 37, 1–174.

Jorissen, F.J., Barmawidjaja, D.M., Puškarić, S., Van der Zwaan, G.J., 1992. Vertical distribution of benthic foraminifera in the northern Adriatic Sea: the relation with the organic flux. Mar. Micropaleontol. 19, 131–146.

Jorissen, F.J.,Wittling, I., Peypouquet, J.P., Rabouille, C., Relexans, J.C., 1998. Live benthic foraminiferal faunas off Cape Blanc NW-Africa: Community structure and microhabitats. Deep-Sea Research 45, 2157–2188.

Kouwenhoven, T.J., Hilgen, F.J., van der Zwaan, G.J., 2003. Late Tortonian–early Messinian stepwise disruption of the Mediterranean–Atlantic connections: constraints from benthic foraminiferal and geochemical data. Palaeogeography, Palaeoclimatology, Palaeoecology 18, 303–319.

Kouwenhoven, T.J., Morigi, C., Negri, A., Giunta, S., Krijgsman, W., Rouchy, J.-M., 2006. Paleoenvironmental evolution of the eastern Mediterranean during the Messinian: Constraints from integrated microfossil data of the Pissouri Basin (Cyprus). Marine Micropaleontology 60, 17-44.

Kouwenhoven, T.J., Seidenkrantz, M.-S., van der Zwaan, G.J., 1999. Deep-water changes: the near-synchronous disappearance of a group of benthic foraminifera from the late Miocene Mediterranean. Palaeogeography, Palaeoclimatology, Palaeoecology 152, 259–281.

Krijgsman,W., Hilgen, F.J., Raffi, I., Sierro, F.J., Wilson, D.S., 1999a. Chronology, causes, and progression of the Messinian salinity crisis. Nature 400, 652–655.

Krijgsman, W., Langereis, C.G., Zachariasse, W.J. Boccaletti, M., Moratti, G. Gelati, R., Iaccarino, S., Papani, G., Villa, G., 1999b. Late Neogene evolution of the Taza–Guercif Basin (Rifian Corridor, Morocco) and implications for the Messinian salinity crisis. Marine Geology 153, 147–160.

Langer, M.R., 1993. Epiphytic foraminifera. Marine Micropaleontology 20, 235–265.

Loeblich Jr., A.R., Tappan, H., 1987. Foraminiferal Genera and Their Classification. 2 Volumes, 1: 970 pp.; 2: 213 pp. 847 pls. Van Reinhold Company, New York.

Lourens, L.J., Hilgen, F.J., Shackleton, N.J., Laskar, J., Wilson, D., 2004. The Neogene Period. In: Gradstein, F., Ogg J. et al. (Eds.), A Geologic Time Scale 2004. Cambridge University Press, Cambridge, pp. 409–430.

Manzi, V., Gennari, R., Hilgen, F., Krijgsman, W., Lugli, S., Roveri, M., Sierro, F.J., 2013. Age refinement of theMessinian salinity crisis onset in theMediterranean. Terra Nova 25, 315–322.

Mariani, E., Parona, C.F., 1887. Fossili tortoniani di Capo S. Marco in Sardegna. Atti Soc. It. Sc. Nat. 30, 101–187.

Martin, J.M., Braga, J.C., 1994. Messinian events in the Sorbas basin in Southeast Spain and their implications in the recent history of the Mediterranean. Sedimentary Geology 90, 257–268.

Mateu-Vicens, G., Khokhlova, A., Sebastián-Pastor, T., 2014. Epiphytic foraminiferal indices as bioindicators in Mediterranean seagrass meadows. Journal of Foraminiferal Research 44, 325–339.

Meijer, P.Th., Krijgsman, W.A., 2005. Quantitative analysis of the desiccation and refilling of the Mediterranean during the Messinian Salinity Crisis. Earth and Planetary Science Letters 240, 510–520.

Milker, Yvonne and Schmiedl, Gerhard, 2012. A taxonomic guide to modern benthic shelf foraminifera of the western Mediterranean Sea. Palaeontologia Electronica Vol. 15, Issue 2;16A,134p; palaeo-electronica.org/content/2012-issue-2-articles/223-taxonomy-foraminifera

Milker, Y., Schmiedl, G., Betzler, C., Römer, M., Jaramillo-Vogel, D., Siccha, M., 2009. Distribution of recent benthic foraminifera in shelf carbonate environments of the Western Mediterranean Sea. Marine Micropaleontology 73, 207–225.

Moissette, P., Saint Martin, J.-P., André, J.-P., Pestrea, S., 2002. L'association microbialite – bryozoaires dans le Messinien de Sicile et de Sardaigne. Geodiversitas 24 (3), 611 – 623.

Mojtahid, M., Griveaud, C., Fontanier, C., Anschutz, P., Jorissen, F.J., 2010. Live benthic foraminiferal faunas along a bathymetrical transect (140–4800 m) in the Bay of Biscay (NE Atlantic). Revue de micropaléontologie 53, 139–162.

Mojtahid, M., Jorissen, F.J., Lansard, B., Fontanier, C., Bombled, B., Rabouille, C., 2009. Spatial distribution of live benthic foraminifera in the Rhône prodelta: Faunal response to a continental-marine organic matter gradient. Marine Micropaleontology 70, 177–200.

Montigny, R., Edel, J.B., Thuizat, R., 1981. Oligo-Miocene rotation of Sardinia: K-Ar ages and paleomagnetic data of Tertiary volcanics. Earth Planet. Sc. Lett. 54, 261–271. doi: 10.1016/0012-821X(81)90009-1

Morigi, C., Negri, A., Giunta, S., Kouwenhoven, T., Krijgsman, W., Blanc-Valleron, M.M., Orszag-Sperber, F., Rouchy, J.-M., 2007. Integrated quantitative biostratigraphy of the latest Tortonian–early Messinian Pissouri section (Cyprus): An evaluation of calcareous plankton bioevents. Geobios 40, 267–279.

Murray, J.W., 1991. Ecology and Paleoecology of Benthic Foraminifera. Longman, Harlow.

Ogniben, L., 1957. Petrografia della Serie Solfifera Siciliana e considerazioni geologiche relative. Memorie Descrittive della Carta Geologica d'Italia 33, 1–275.

Pecorini, G., 1972. La trasgressione pliocenica di Capo S. Marco (Oristano, Sardegna occidentale). Boll. Soc. Geol. It. 91, 365–372.

Pérez-Asensio, J.N., Aguirre, J., Jiménez-Moreno, G., Schmiedl, G., Civis, J., 2013. Glacioeustatic control on the origin and cessation of the Messinian salinity crisis. Global and Planetary Change, 111, 1–8, http://dx.doi.org/10.1016/j.gloplacha.2013.08.008.

Pérez-Asensio, J.N., Aguirre, J., Schmiedl, G., Civis, J., 2012a. Impact of restriction of the Atlantic-Mediterranean gateway on the Mediterranean Outflow Water and eastern Atlantic circulation during the Messinian. Paleoceanography 27, PA3222. doi:10.1029/2012PA002309.

Pérez-Asensio, J.N., Aguirre, J., Schmiedl, G., Civis, J., 2012b. Messinian paleoenvironmental evolution in the lower Guadalquivir Basin (SW Spain) based on benthic foraminifera. Palaeogeography, Palaeoclimatology, Palaeoecology 326–328, 135–151.

Pérez-Asensio, J.N., Aguirre, J., Schmiedl, G., Civis, J., 2014. Messinian productivity changes in the northeastern Atlantic and their relationship to the closure of the Atlantic–Mediterranean gateway: implications for Neogene palaeoclimate and palaeoceanography. J. Geol. Soc. London 171, 389–400.

Raffi, I., Mozzato, C., Fornaciari, E., Hilgen, F.J., Rio, D., 2003. Late Miocene calcareous nannofossil biostratigraphy and astrobiochronology for the Mediterranean region. Micropaleontology 49, 1–26.

Retailleau, S., Howa, H., Schiebel, R., Lombard, F., Eynaud, F., Schmidt, S., Jorissen, F., Labeyrie, L., 2009. Planktic foraminiferal production along an offshore-onshore transect in the south-eastern Bay of Biscay. Continental Shelf Research 29, 1123–1135.

Riding, R., Braga, J.C., Martín, J.M., Sanchez-Almazo, I.M., 1998. Mediterranean Messinian Salinity Crisis: constraints from a coeval marginal basin, Sorbas, southeastern Spain. Sedimentary Geology 146, 1–20.

Rouchy, J.M., 1980. La genése des évaporites messiniennes de Méditerranée: un bilan. Bull. Cent. Rech. Explor. Prod. Elf Aquitaine 4, 511–545.

Rouchy, J.M., Caruso, A., 2006. The Messinian salinity crisis in the Mediterranean Basin: a reassessment of the data and an integrated interval. Sediment. Geol. 188–189, 35–67.

Roveri, M., Flecker, R., Krijgsman, W., Lofi, J., Lugli, S., Manzi, V., Sierro, F.J., Bertini, A., Camerlenghi, A., De Lange, G., Govers, R., Hilgen, F.J., Hübscher, C., Meijer, P.Th., Stoica, M., 2014. The Messinian Salinity Crisis: Past and future of a great challenge for marine sciences. Marine Geology 352, 25–58.

Roveri, M., Gennari, R., Lugli, S., Manzi, V., 2009. The Terminal Carbonate Complex: the record of sea-level changes during the Messinian salinity crisis. GeoActa 8, 57–71.

Ruggieri, G., 1967. The Miocene and later evolution of the Mediterranean Sea. In: Adams, C.G., Ager, A.V. (Eds.), Aspects of Tethyan Biogeography, 7. Systematics Association Publ., London, pp. 283–290.

Ruiz, F., González-Regalado, M.L., Abad, M., Muñoz, J.M., Pino, R., 2007. New applications of the Poisson distribution in micropalaeontology: relationships between environmental variables and the *Ammonia tepida* distribution in the south-western Spanish estuaries. Terra Nova 19, 367–372.

Ryan, W.B.F., 2009. Decoding the Mediterranean salinity crisis. Sedimentology 56, 95–136.

Sage, F., Von Gronefeld, G., Décerchère, J., Gaullier, V.,Maillard, A., Gorini, C., 2005. Seismic evidence for Messinian detrital deposits at the western Sardinia margin, northwestern Mediterranean. Mar. Petrol. Geol. 22, 757–773.

Saint Martin, J.-P., 2010. The *Girvanella*-like remains from Messinian marine deposits (Sardinia, Italy): Lagerstätten paradigm for microbial biota? Annales de Paléontologie 96, 33–50.

Salvi, G., Buosi, C., Arbulla, D., Cherchi, A., De Giudici, G., Ibba, A., De Muro, S., 2015. Ostracoda and foraminifera response to a contaminated environment: the case of the ex-military arsenal of the La Maddalena Harbour (Sardinia, Italy). Micropaleontology 61 (1–2), 115–133.

Sánchez-Almazo, I.M., Spiro, B., Braga, J.C., Martín, J.M., 2001. Constraints of stable isotope signatures on the depositional palaeoenvironments of upper Miocene reef and temperate carbonates in the Sorbas Basin, SE Spain. Palaeogeography, Palaeoclimatology, Palaeoecology 175, 153-172.

Schmiedl, G., Mackensen, A., Miller, P.J., 1997. Recent benthic foraminifera from the South Atlantic Ocean: dependence on food supply and water masses. Marine Micropaleontology 32, 249–287.

Selli, R., 1954. Il Bacino del Metauro. Giornale di Geologia 24, 1–294.

Selli, R., 1960. Il Messiniano Mayer-Eymar 1867. Proposta di un neostratotipo. Giornale di Geologia 28, 1–33.

Sgarrella, F., Moncharmont Zei, M., 1993. Benthic foraminifera in the Gulf of Naples (Italy): systematics and autoecology. Bollettino della Societá Paleontologica Italiana 32, 145–264.

Shannon, C.E., Weaver, W., 1963. Mathematical Theory of Communication. University of Illinois Press, Urbana.

Sierro, F.J., Flores, J.A., Civis, J., González-Delgado, J.A., Francés, G., 1993. Late Miocene globorotaliid event-stratigraphy and biogeography in the NE-Atlantic and Mediterranean. Mar. Micropaleontol. 21, 143–168.

Sierro, F.J., Flores, J.A., Zamarreno, I., Vazquez, A., Utrilla, R., Frances, G., Hilgen, F., Krijgsman, W., 1997. Astronomical cyclicity and sapropels in the pre-evaporitic Messinian of the Sorbas basin (Western Mediterranean). Geogaceta 21, 199–202.

Sierro, F.J., Flores, J.A., Francés, G., Vazquez, A., Utrilla, R., Zamarreño, I., Erlenkeuser, H., Barcena, M.A., 2003. Orbitally controlled oscillations in planktic communities and cyclic changes in western Mediterranean hydrography during the Messinian. Palaeogeography, Palaeoclimatology, Palaeoecology 190, 289–316.

Sierro, F.J., Flores, J.A., Zamarreño, I., Vazquez, A., Utrilla, R., Frances, G., Hilgen, F.J., Krijgsman, W., 1999. Messinian pre-evaporite sapropels and precession-induced oscillations in western Mediterranean climate. Marine Geology 153, 137–146.

Sjoerdsma, P.G., Van der Zwaan, G.J., 1992. Simulating the effect of changing organic flux and oxygen content on the distribution of benthic foraminifera. Marine Micropaleontology 19, 163–180.

Van Couvering, J.A., Castradori, D., Cita, M.B., Hilgen, F.J., Rio, D., 2000. The base of the Zanclean Stage and of the Pliocene Series. Episodes 23, 179–187.

Van Hoey, G., Vincx, M., Degraer, S., 2005. Small- to large-scale geographical patterns within the macrobenthic *Abra alba* community. Estuarine, Coastal and Shelf Science 64, 751–763.

Van der Zwaan, G.J., 1982. Paleoecology of Late Miocene foraminifera. Utrecht Micropaleontological Bulletin 25, 1–201.

Violanti, D., 1996. Paleoautecological analysis of *Bulimina echinata* (Messinian, Mediterranean area). In: Cherchi, A. (Ed.), Autecology of Selected Fossil Organisms. Bolletino della Societa Paleontologica Italiana 3, 243–253.

Violanti, D., Lozar, F., Natalicchio, M., Dela Pierre, F., Bernardi, E., Clari, P., Cavagna, S., 2013. Stress-tolerant microfossils of a Messinian succession from the Northern Mediterranean basin (Pollenzo section, Piedmont, northwestern Italy). Bollettino della Società Paleontologica Italiana 52, 45-54.

Zettler, M.L., Proffitt, C.E., Darr, A., Degraer, S., Devriese, L., Greathead, C., Kotta, J., Magni, P., Martin, G., Reiss, H., Speybroeck, J., Tagliapietra, D., Van Hoey, G., Ysebaert T., 2013. On the myths of indicator species: issues and further consideration in the use of static concepts for ecological applications. PLoS ONE 8(10), e78219. doi:10.1371/journal.pone.0078219

Figure captions

Fig. 1. A. Distribution of Messinian evaporites in the western Mediterranean Basin (modified from Roveri et al., 2014). B. Location of Cenozoic outcrops in the southern Sinis Peninsula, showing the

studied sections: Capo San Marco (Section A) and Monte Palla (Section B). C. Stratigraphic logs of the sampled Capo San Marco (A) and Monte Palla (B) sections. Simplified lithology: (1) sandstones; (2) muddy siltstones; (3) mudstones; (4) marls; (5) marly and bioclastic limestones; (6) brecciated limestones and dolostones; (7) microbial mounds; (8) laminated limestones; (9) paleosoils; (10) basalt. (PF) Planktonic foraminifera; (CN) Calcareous Nannoplankton; (FM) Formations; (Sa) Sapropelithic layers; (MM) Microbial Mound; (Mc) Microbial crust; (P) Paleosoil; (H) Hiatus; (MES) Messinian Erosional Surface. T/M boundary is reported. Basaltic flow is dated at 4.83-4.58 Ma (Duncan et al., 2011).

Fig. 2. A) Western side of the Capo San Marco cliff. The upper part of the CSMF is partially eroded below the SLLF. These formations are separated by montimorillonitic paleosoils. B) Western side of the Capo San Marco cliff. Unconformity between SLLF (bottom) and TSF, brecciated and arranged in chaotic features.

Fig. 3. Panoramic view of the western side of the Capo San Marco section, showing the uppermost Tortonian marls (T) covered by Messinian units (M).

Fig. 4. Distribution of selected planktonic foraminiferal species and calcareous nannofossils from the Capo San Marco and Monte Palla sections (from Cherchi and Martini, 1981). (PF) Planktonic foraminifera; (CN) Calcareous Nannoplankton; (FM) Formation. T/M boundary is reported.

Fig. 5. Quantitative distribution patterns of selected benthic foraminiferal species (with a relative abundance >3% in at least 3 samples). The grey lines indicate the five-time intervals of benthic foraminifera barren of the studied sections.

Fig. 6. Quantitative distribution of selected palaeodiversity indices and the ecological preferences of benthic foraminifera (percentages of the total species): potential epiphytes; nutrient-enriched conditions species; and potential low salinity species. The grey lines indicate the five-time intervals of benthic foraminifera barren of the studied sections.

Fig. 7. Dendrogram based on Q-mode Hierarchical Cluster Analysis based on Euclidean-distance correlation coefficients (Ward's linkage method).

Fig. 8. Representation of the three first components of the Principal Components Analysis (PCA) carried out on the selected benthic foraminiferal species (with a relative abundance >3% in at least 3

sample). A) Component 1 vs Component 2; B) Component 1 vs Component 3; C) eigenvalues of components.

Fig. 9. Representation of MSC stages (according to Roveri et al., 2014) and three palaeoecological intervals (A-B-C), which are characterized by different palaeobiocoenosis. Light grey lines indicate the five-time intervals of fossils barren.

Table captions

Table 1. Inferred biochronology based on selected planktonic species from the Sinis Messinian Basin, based on bibliographical data. FO (First Occurrence); LO (Last Occurrence); FCO (First Common Occurrence); LCO (Last Common Occurrence); PE (Paracme End); S/D (Sin/Dx coiling change).

Table 2. Range values of relative abundance of main benthic foraminifera species, ecological groups and biotic indices of the 4 clusters identified in the studied area.

Supplementary materials

Appendix A. List of modern ecological information and environmental distribution of the dominant benthic foraminiferal species studied in the Capo San Marco and Monte Palla sections.

Appendix B. List of benthic foraminiferal species studied in the Capo San Marco and Monte Palla sections.

Fig. 1

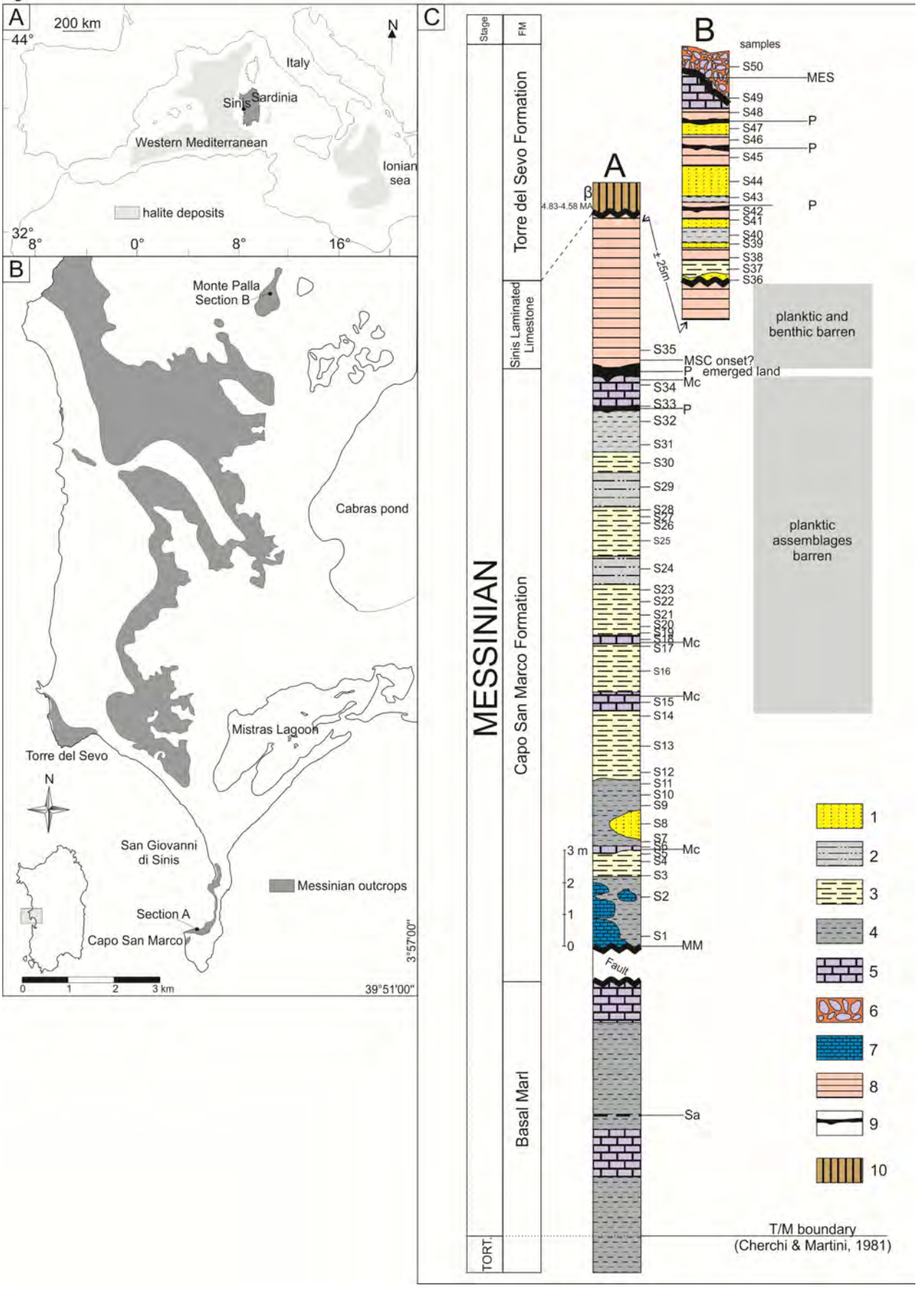
A
200 km
N
44°
Italy
Sinis
Sardinia
Western Mediterranean
Ionian sea
halite deposits
32°
8°
0°
8°
16°
B
Monte Palla Section B
Cabras pond
Mistras Lagoon
Torre del Sevo
N
San Giovanni di Sinis
Messinian outcrops
Section A
Capo San Marco
3°57'00"
0 1 2 3 km
39°51'00"
C
Stage
FM
MESSINIAN
Torre del Sevo Formation
Sinis Laminated Limestone
Capo San Marco Formation
Basal Marl
TORT.
A
β
4.83-4.58 MA
± 25m
3 m
2
1
0
Fault
Sa
B
samples
S50
MES
S49
S48
S47
P
S46
P
S45
S44
S43
P
S42
S41
S40
S39
S38
S37
S36
planktic and benthic barren
S35
MSC onset?
P emerged land
S34
Mc
S33
P
S32
S31
S30
S29
S28
S27
S26
S25
S24
S23
S22
S21
S20
S19
S18
S17
Mc
S16
S15
Mc
S14
S13
S12
S11
S10
S9
S8
S7
S6
S5
Mc
S4
S3
S2
S1
MM
planktic assemblages barren
1
2
3
4
5
6
7
8
9
10
T/M boundary
(Cherchi & Martini, 1981)

Fig. 2

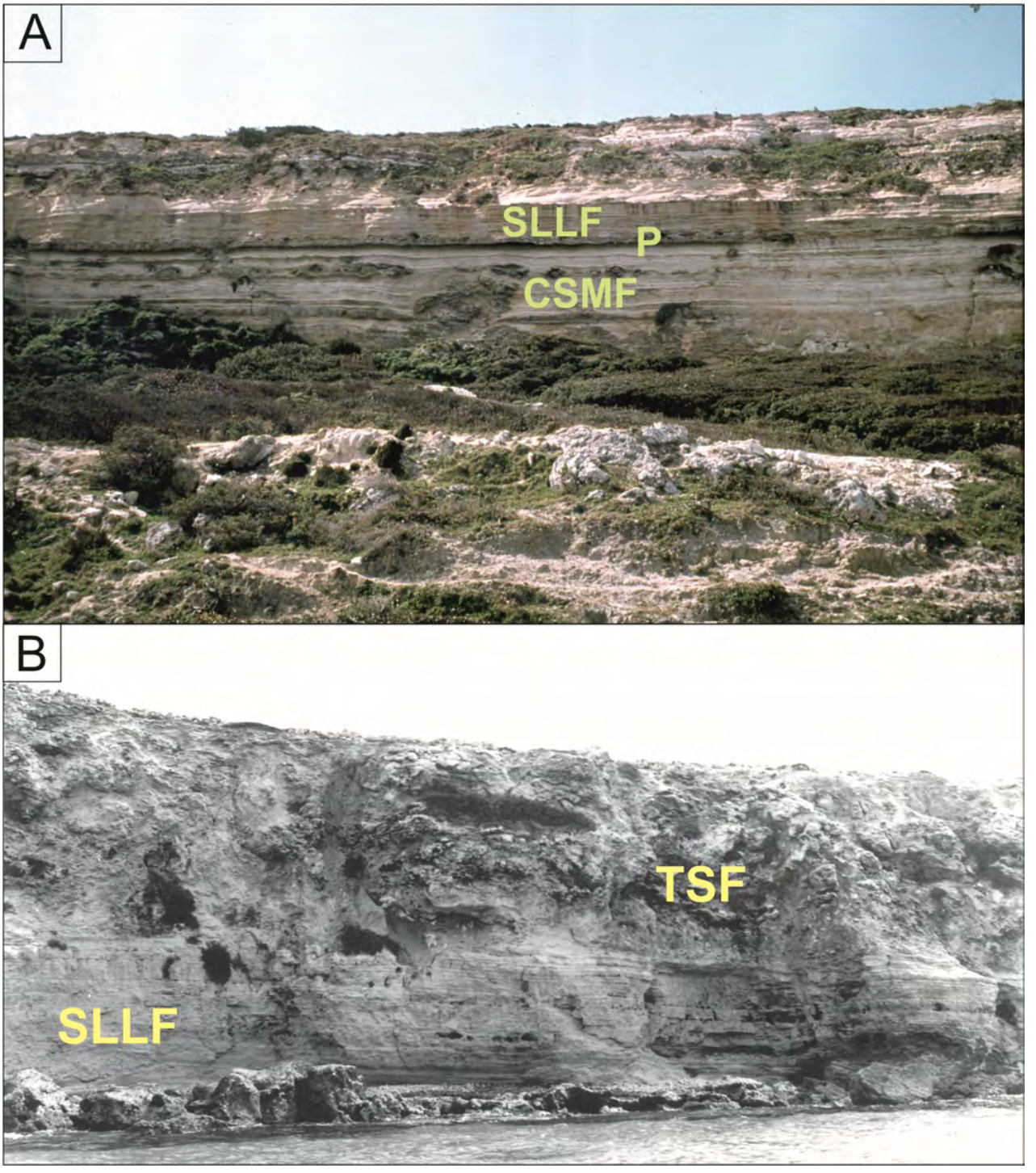

Fig. 3

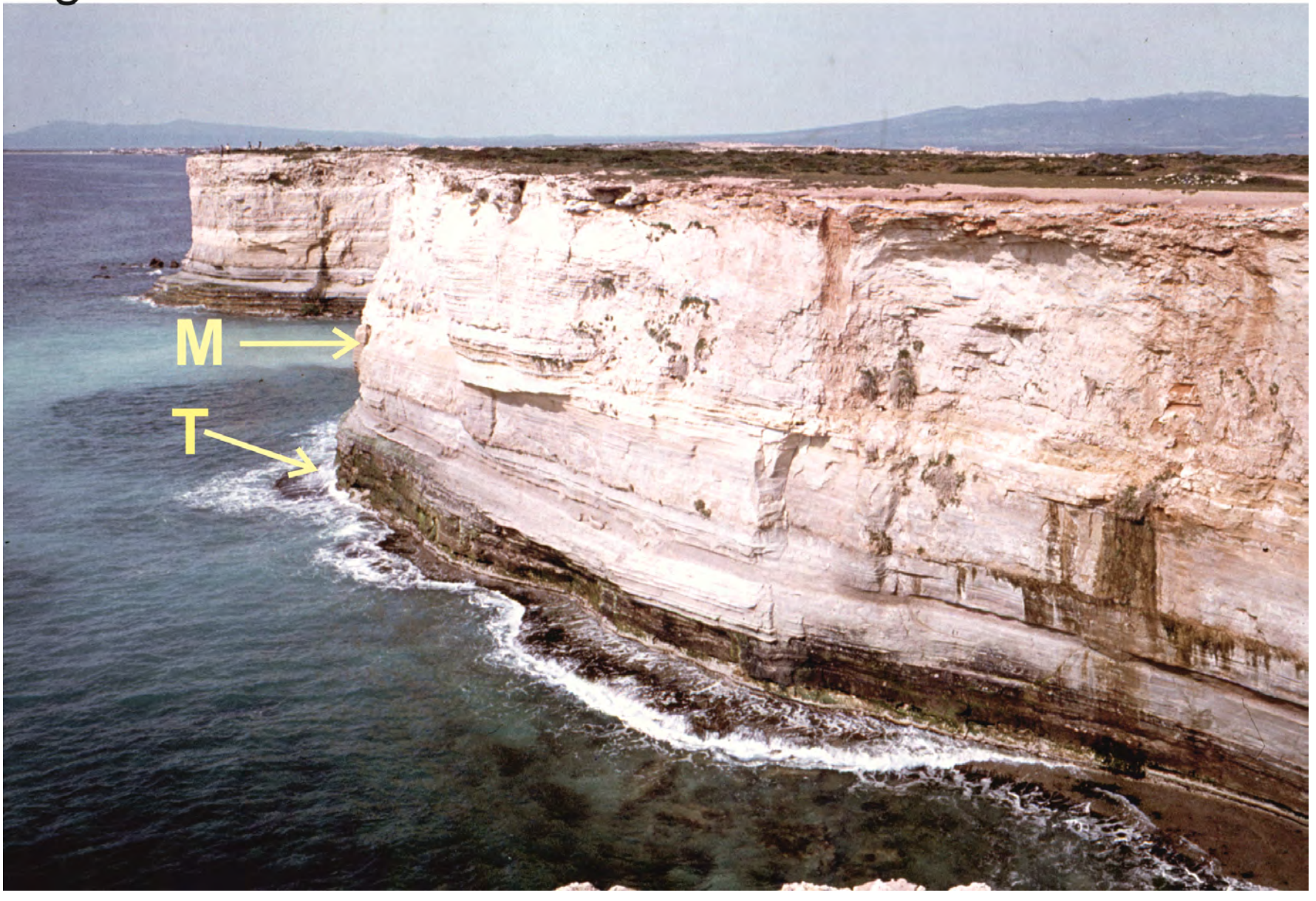

Fig. 4

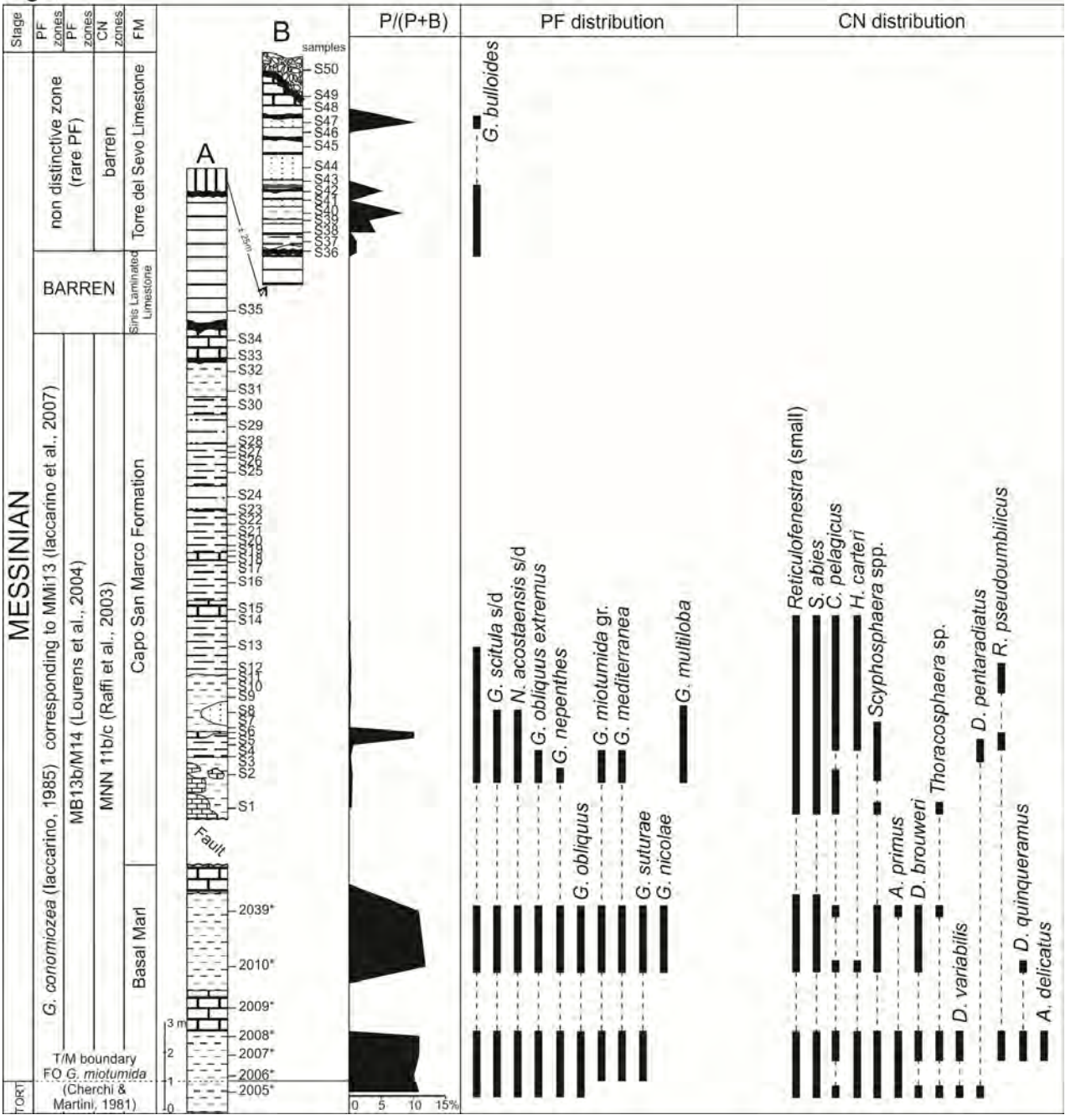
Stage
PF zones
PF zones
CN zones
FM
MESSINIAN
TORT
G. conomiozea (Iaccarino, 1985) corresponding to MMi13 (Iaccarino et al., 2007)
MB13b/M14 (Lourens et al., 2004)
MNN 11b/c (Raffi et al., 2003)
T/M boundary
FO G. miotumida
(Cherchi & Martini, 1981)
BARREN
non distinctive zone (rare PF)
barren
Basal Marl
Capo San Marco Formation
Sinis Laminated Limestone
Torre del Sevo Limestone
A
B
samples
Fault
P/(P+B)
PF distribution
CN distribution
G. bulloides
G. scitula s/d
N. acostaensis s/d
G. obliquus extremus
G. nepenthes
G. obliquus
G. miotumida gr.
G. mediterranea
G. sutural
G. nicolae
G. multiloba
Reticulofenestra (small)
S. abies
C. pelagicus
H. carteri
Scyphosphaera spp.
A. primus
D. brouweri
Thoracosphaera sp.
D. variabilis
D. pentaradiatus
R. pseudoumbilicus
D. quinqueramus
A. delicatus

Fig. 5

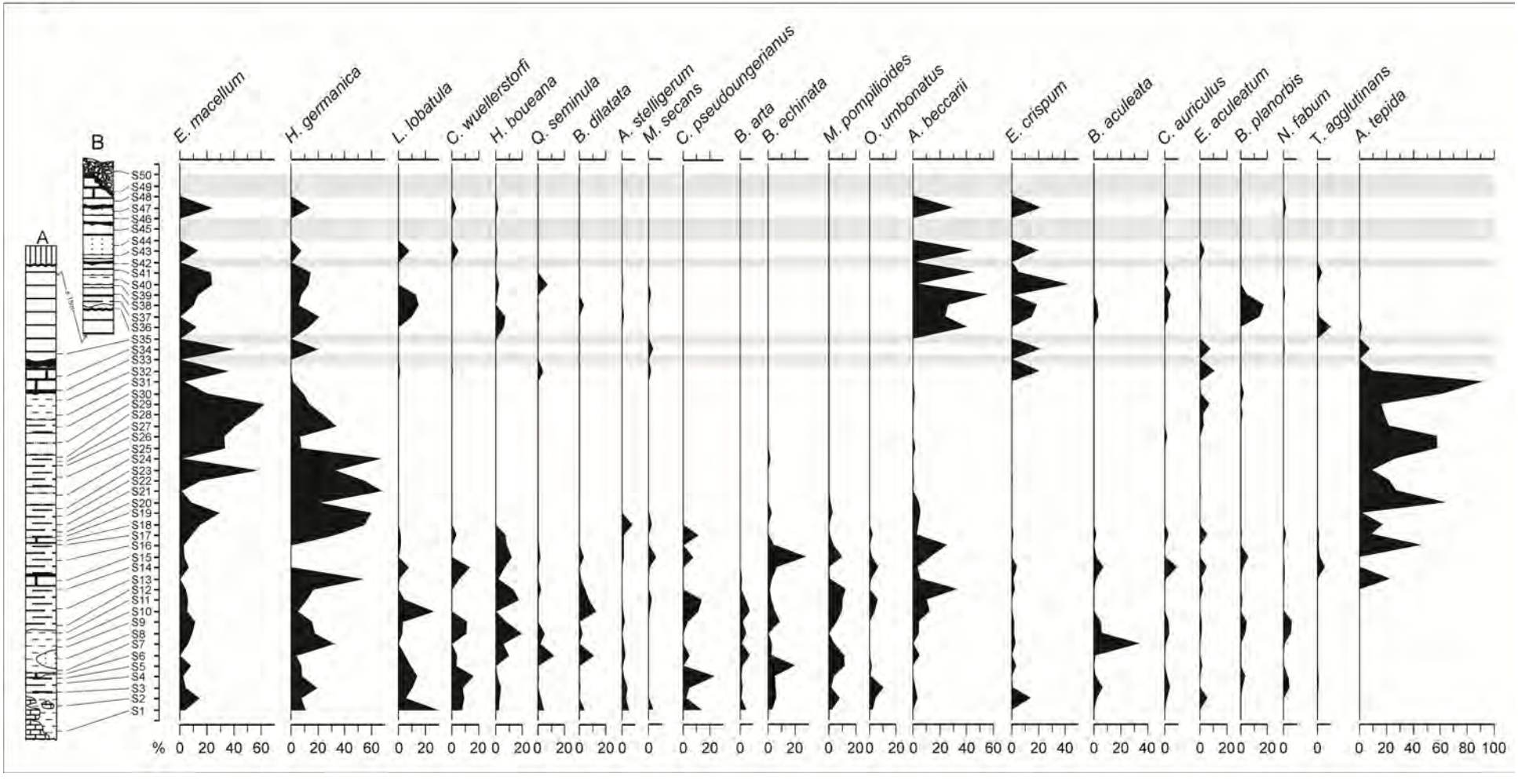
A
B
E. macellum
H. germanica
L. lobatula
C. wuellerstorfi
H. boueana
Q. seminula
B. dilatata
A. stelligerum
M. secans
C. pseudoungerianus
B. arta
B. echinata
M. pompilioides
O. umbonatus
A. beccarii
E. crispum
B. aculeata
C. auriculus
E. aculeatum
B. planorbis
N. fabum
T. agglutinans
A. tepida
S50
S49
S48
S47
S46
S45
S44
S43
S42
S41
S40
S39
S38
S37
S36
S35
S34
S33
S32
S31
S30
S29
S28
S27
S26
S25
S24
S23
S22
S21
S20
S19
S18
S17
S16
S15
S14
S13
S12
S11
S10
S9
S8
S7
S6
S5
S4
S3
S2
S1
%
0 20 40 60
0 20 40 60
0 20
0 20
0 200
0 200
0 200
0 200
0 0
0 0
0 20
0 0
0 20
0 200
0 200
0 20 40 60
0 20 40
0 20 40
0 200
0 200
0
0 20 40 60 80 100

Figure 6

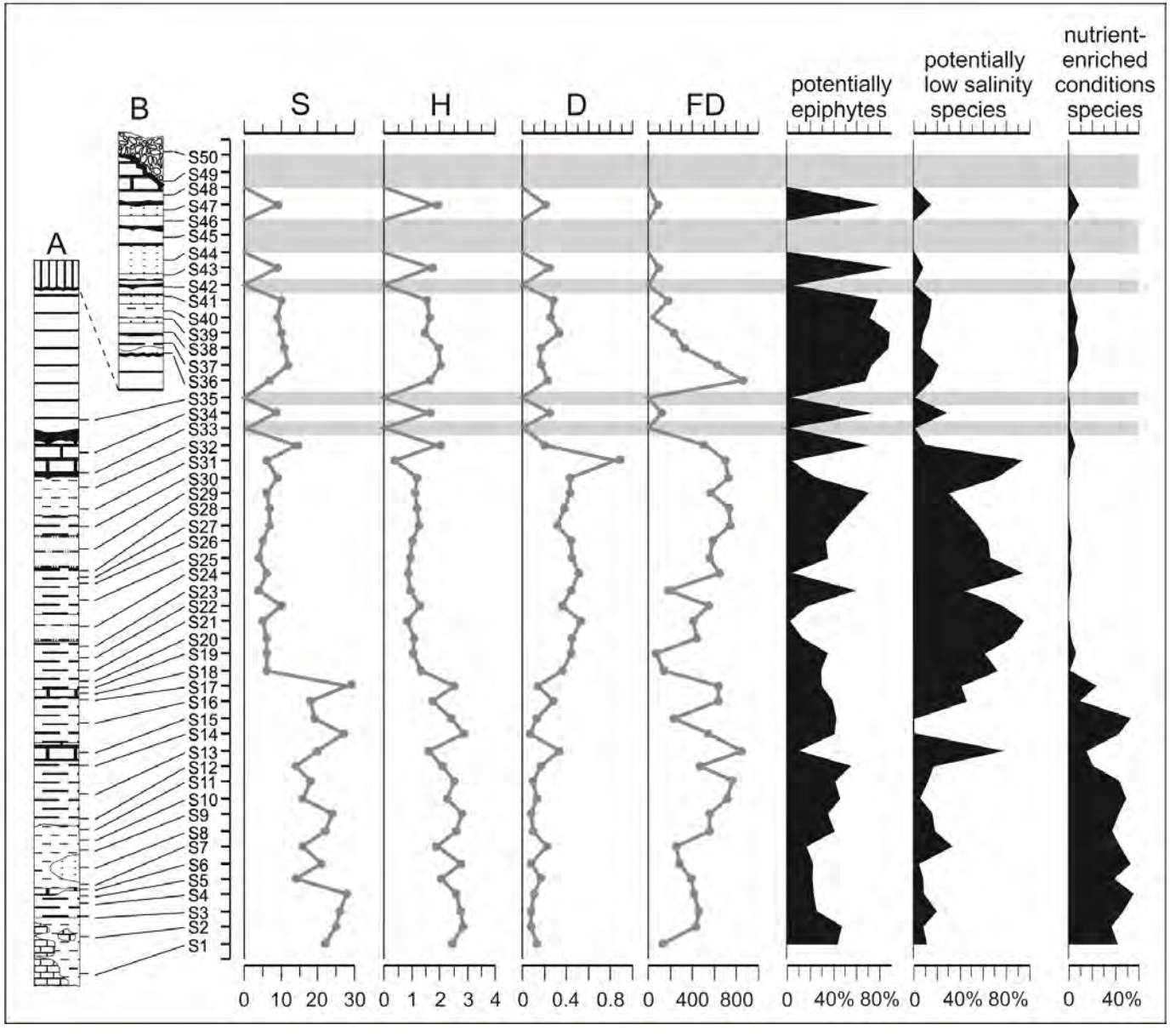
A
B
S
H
D
FD
potentially epiphytes
potentially low salinity species
nutrient-enriched conditions species
S50
S49
S48
S47
S46
S45
S44
S43
S42
S41
S40
S39
S38
S37
S36
S35
S34
S33
S32
S31
S30
S29
S28
S27
S26
S25
S24
S23
S22
S21
S20
S19
S18
S17
S16
S15
S14
S13
S12
S11
S10
S9
S8
S7
S6
S5
S4
S3
S2
S1
0 10 20 30
0 1 2 3 4
0 0.4 0.8
0 400 800
0 40% 80%
0 40% 80%
0 40%

Figure 7

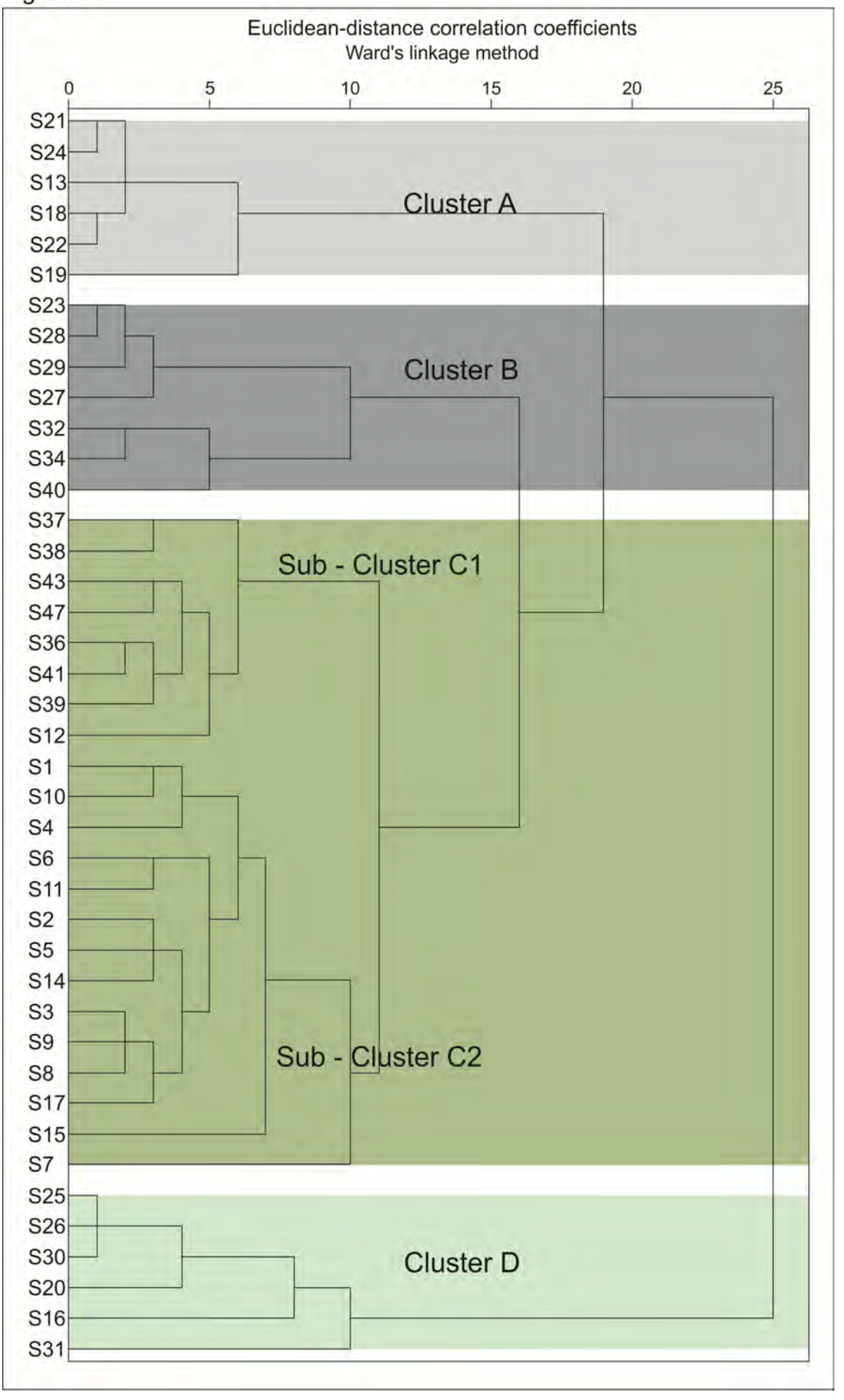
Euclidean-distance correlation coefficients
Ward's linkage method
0
5
10
15
20
25
S21
S24
S13
S18
S22
S19
S23
S28
S29
S27
S32
S34
S40
S37
S38
S43
S47
S36
S41
S39
S12
S1
S10
S4
S6
S11
S2
S5
S14
S3
S9
S8
S17
S15
S7
S25
S26
S30
S20
S16
S31
Cluster A
Cluster B
Sub - Cluster C1
Sub - Cluster C2
Cluster D

Fig. 8

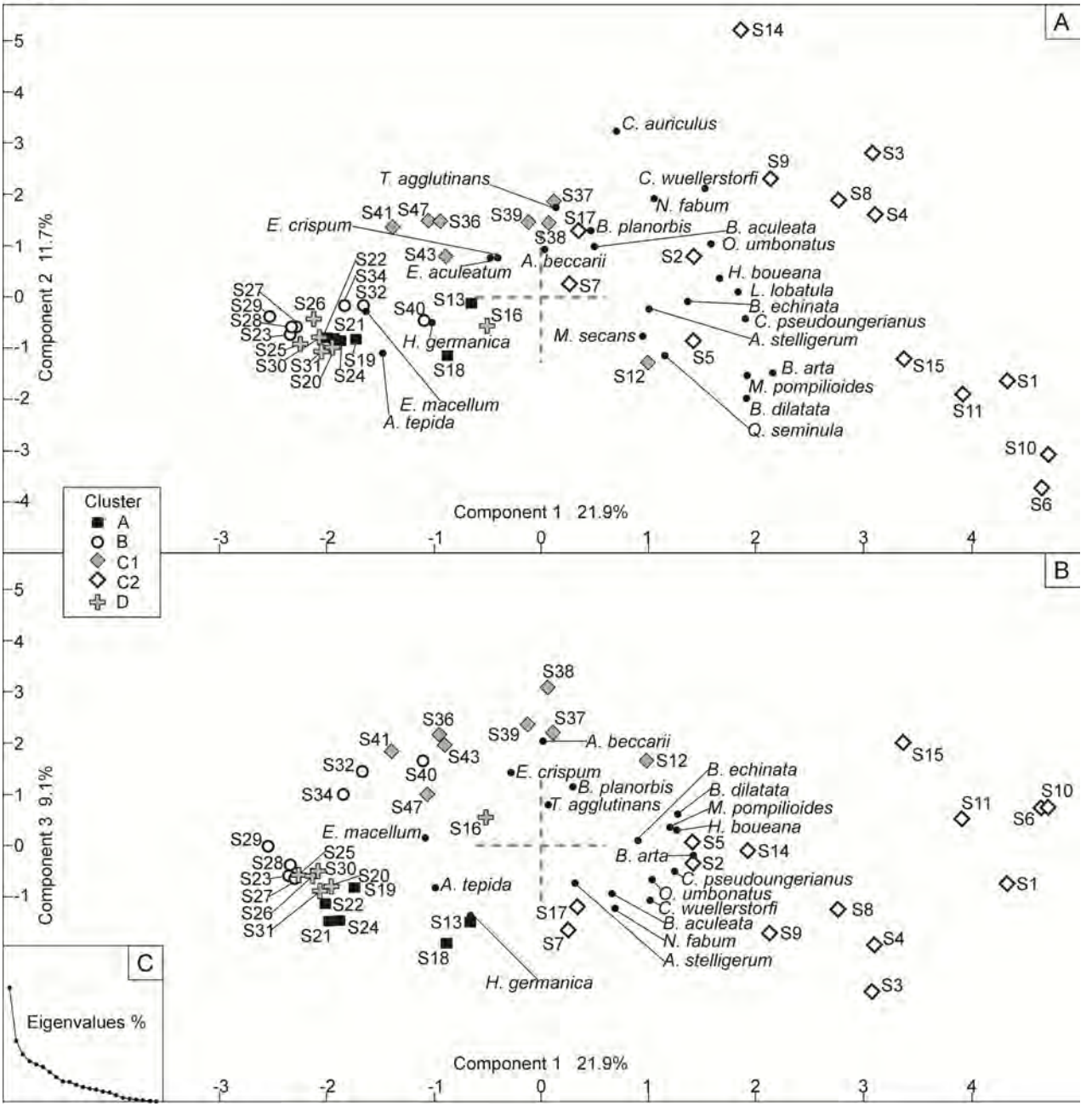
A
B
C
Component 1 21.9%
Component 2 11.7%
Component 3 9.1%
Cluster
A
B
C1
C2
D
Eigenvalues %
S14
C. auriculus
S3
S9
C. wuellerstorfi
T. agglutinans
S37
N. fabum
S8
S41
S47
S36
S39
S17
B. planorbis
B. aculeata
S4
E. crispum
S38
O. umbonatus
S43
A. beccarii
S2
S22
E. aculeatum
H. boueana
S34
S7
L. lobatula
S27
S32
B. echinata
S29
S26
S40
S13
S16
C. pseudoungerianus
S28
S21
H. germanica
M. secans
A. stelligerum
S23
S5
S25
S19
S18
S12
S15
B. arta
S30
S31
S24
M. pompilioides
S1
S20
E. macellum
S11
B. dilatata
A. tepida
Q. seminula
S10
S6
S38
S36
S37
S39
S41
A. beccarii
S43
S12
S15
S32
S40
E. crispum
B. echinata
S10
S34
B. planorbis
B. dilatata
S11
S47
T. agglutinans
M. pompilioides
S6
S29
S16
H. boueana
E. macellum
S5
S14
S25
B. arta
S28
S30
S2
S1
S23
S20
C. pseudoungerianus
A. tepida
S27
S19
O. umbonatus
S26
S22
S17
S8
C. wuellerstorfi
S31
S24
S13
B. aculeata
S9
S21
S7
N. fabum
S4
S18
A. stelligerum
H. germanica
S3

Fig. 9

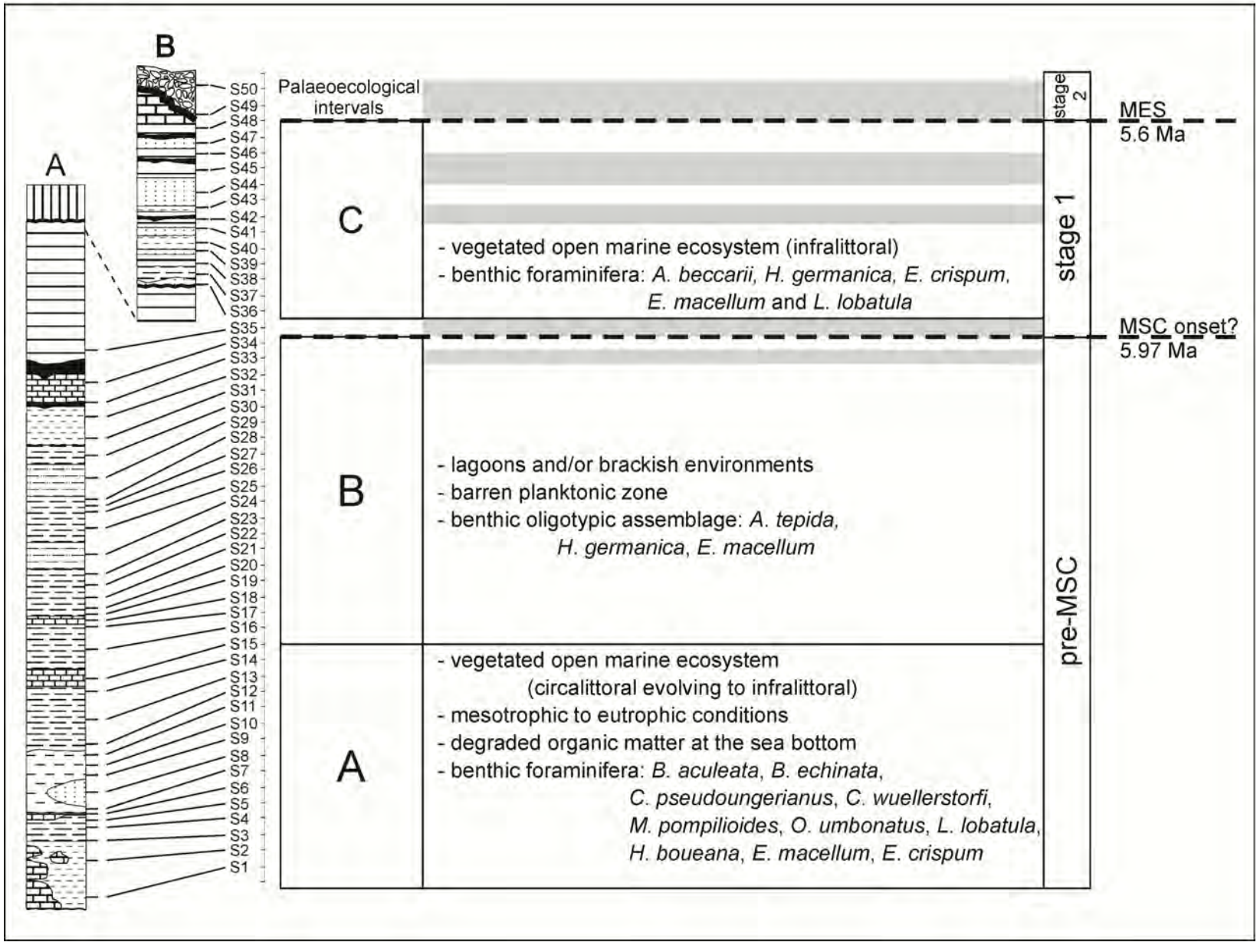
B
A
S50
S49
S48
S47
S46
S45
S44
S43
S42
S41
S40
S39
S38
S37
S36
S35
S34
S33
S32
S31
S30
S29
S28
S27
S26
S25
S24
S23
S22
S21
S20
S19
S18
S17
S16
S15
S14
S13
S12
S11
S10
S9
S8
S7
S6
S5
S4
S3
S2
S1
Palaeoecological intervals
C
- vegetated open marine ecosystem (infralittoral)
- benthic foraminifera: A. beccarii, H. germanica, E. crispum, E. macellum and L. lobatula
B
- lagoons and/or brackish environments
- barren planktonic zone
- benthic oligotypic assemblage: A. tepida, H. germanica, E. macellum
A
- vegetated open marine ecosystem (circalittoral evolving to infralittoral)
- mesotrophic to eutrophic conditions
- degraded organic matter at the sea bottom
- benthic foraminifera: B. aculeata, B. echinata, C. pseudoungerianus, C. wuellerstorfi, M. pompilioides, O. umbonatus, L. lobatula, H. boueana, E. macellum, E. crispum
stage 2
stage 1
pre-MSC
MES
5.6 Ma
MSC onset?
5.97 Ma